Received: 14 December 2023 | Revised: 26 April 2024 | Accepted: 24 May 2024

DOI: 10.1111/bph.16483

RESEARCH ARTICLE

Inhibition of proline-rich tyrosine kinase 2 restores cardioprotection by remote ischaemic preconditioning in type 2 diabetes

Ralf Erkens[1] | Dragos Andrei Duse[1] | Amanda Brum[1] | Alexandra Chadt[2,3] | Stefanie Becher[1] | Mauro Siragusa[4,5] | Christine Quast[1] | Johanna Müssig[1] | Michael Roden[3,6,7] | Miriam Cortese-Krott[1,8] | Borja Ibáñez[9] | Eckhard Lammert[3,10] | Ingrid Fleming[4,5] | Christian Jung[1] | Hadi Al-Hasani[2,3] | Gerd Heusch[11] | Malte Kelm[1,8]

Correspondence
Ralf Erkens and Malte Kelm, Department of Cardiology, Pulmonology and Vascular Medicine, Medical Faculty, Heinrich Heine University of Düsseldorf, Moorenstraße 5, 40225 Düsseldorf, Germany.
Email: ralf.erkens@med.uni-duesseldorf.de and malte.kelm@med.uni-duesseldorf.de

Funding information
This work was supported by the German Research Council (CRC 1116 to C.J., M.K., G.H., SFB 1366/2 B01, Project ID 394046768 to I.F.); by a research grant from the Forschungskommission, Medical Faculty of the Heinrich Heine University Duesseldorf (Grant No. 2018-50 to R.E. and No. 2022-01 to D.A.D.); and by the Christiane and Claudia Hempel Foundation (to R.E.). Additionally, some of the presented work in this study is part of the RESILIENCE (European Union's Horizon 2020 research and innovation program, grant No.: 945118 to B.I. and M.K.).

Abstract

Background and Purpose: Remote ischaemic preconditioning (rIPC) for cardioprotection is severely impaired in diabetes, and therapeutic options to restore it are lacking. The vascular endothelium plays a key role in rIPC. Given that the activity of endothelial nitric oxide synthase (eNOS) is inhibited by proline-rich tyrosine kinase 2 (Pyk2), we hypothesized that pharmacological Pyk2 inhibition could restore eNOS activity and thus restore remote cardioprotection in diabetes.

Experimental Approach: New Zealand obese (NZO) mice that demonstrated key features of diabetes were studied. The consequence of Pyk2 inhibition on endothelial function, rIPC and infarct size after myocardial infarction were evaluated. The impact of plasma from mice and humans with or without diabetes was assessed in isolated buffer perfused murine hearts and aortic rings.

Key Results: Plasma from nondiabetic mice and humans, both subjected to rIPC, caused remote tissue protection. Similar to diabetic humans, NZO mice demonstrated endothelial dysfunction. NZO mice had reduced circulating nitrite levels, elevated arterial blood pressure and a larger infarct size after ischaemia and reperfusion than BL6 mice. Pyk2 increased the phosphorylation of eNOS at its inhibitory site (Tyr656), limiting its activity in diabetes. The cardioprotective effects of rIPC were abolished in diabetic NZO mice. Pharmacological Pyk2 inhibition restored endothelial function and rescued cardioprotective effects of rIPC.

Abbreviations: AMI, acute myocardial infarction; BL6, C57BL/6; cPTIO, 2-4-carboxyphenyl-4,4,5,5-tetramethylimidazoline-1-oxyl-3-oxide; DM, diabetes mellitus; $eNOS^{-/-}$ mice, endothelial nitric oxide synthase-knockout mice; FMD, flow-mediated dilation; LV, left ventricle; LVEDP, left-ventricular end-diastolic pressure; NZO, New Zealand obese mice; Phe, phenylephrine; PI3K, phosphatidylinositol 3-kinase; rIPC, remote ischaemic preconditioning; SNP, sodium nitroprusside.

Ralf Erkens and Dragos Andrei Duse should be considered joint first author.

An earlier version of this manuscript was uploaded to the preprint server bioRxiv (bioRxiv 2023. doi: 10.1101/2023.04.25.538211).

For affiliations refer to page 4191

Conclusion and Implications: Endothelial function and remote tissue protection are impaired in diabetes. Pyk2 is a novel target for treating endothelial dysfunction and restoring cardioprotection through rIPC in diabetes.

KEYWORDS
acute myocardial infarction, diabetes, endothelial dysfunction, endothelial function, eNOS, Pyk2, remote ischaemic preconditioning

1 | INTRODUCTION

Diabetes mellitus (DM) is associated with a three-fold elevated risk of myocardial infarction (Kalyani, 2021), but distinct subtypes and endotypes of DM carry different cardiovascular risks (Ahlqvist et al., 2018; Zaharia et al., 2019). Specifically, severe insulin-resistant diabetes is associated with the highest cardiovascular risk and experience the worst outcomes. Humans with type 2 DM and acute myocardial infarction (AMI) have larger infarct sizes and greater impairment of left ventricular (LV) function than those without diabetes, associated with distinct patterns in the myocardial texture (Reinstadler et al., 2017). Such humans would be expected to particularly benefit from specific strategies to reduce the infarct size after AMI (Milazzo et al., 2021; Sarwar et al., 2010). One strategy reported to have a cardioprotective effect is remote ischaemic preconditioning (rIPC) (Heusch, 2020), but unfortunately, the effect of this approach seems to be impaired in humans with diabetes (Ferdinandy et al., 2023; Hausenloy et al., 2019). Strategies to restore the effectiveness of rIPC are lacking (Feige et al., 2022; Heusch, 2020), largely because the mechanisms underlying its protective effects are unclear. Recently ambiguous outcomes regarding the efficacy of the rIPC manoeuvre performed under controlled preclinical conditions have been reported (Sayour et al., 2023). Neuronal, humoral and endothelial pathways have been postulated (Ferdinandy et al., 2023; Heusch et al., 2015; Kleinbongard et al., 2017). One key pathway involves the endothelial nitric oxide (NO) synthase (**eNOS**) and its downstream signalling pathways (Rassaf et al., 2014). The factors that regulate eNOS are numerous and include changes in intracellular Ca^{2+} and the substrate L-arginine levels as well as posttranslational modifications. For example, several well-documented phosphorylation sites in eNOS regulate its enzymatic activity. The best studied phosphorylation sites are Ser1177 (human sequence), which can increase eNOS activity and threonine 495 (Thr495), which exerts an inhibitory effect and has to be dephosphorylated for Ca^{2+} and calmodulin to bind and activate the enzyme (Fleming et al., 2001). Less is known about the tyrosine phosphorylation of eNOS, even though it possibly has a more pronounced effect on NO production. There are at least two reported tyrosine residues in eNOS that can be phosphorylated, that is, Tyr83, which has a small effect on eNOS activity (Fulton et al., 2008) and may play a role in protein proteins interactions, and Tyr657 (Tyr656 in mice), the phosphorylation of which completely abrogates NO production (Fisslthaler et al., 2008; Siragusa & Fisslthaler, 2017). The phosphorylation of eNOS on Tyr657 underlines the endothelial dysfunction induced by tonic insulin receptor activation (Fisslthaler et al., 2008; Siragusa & Fisslthaler, 2017). This occurs because even though insulin activates protein kinase B (**Akt**) to phosphorylate Ser1177, any positive effect on NO generation is undermined by the phosphorylation of Tyr657 by Proline-rich tyrosine kinase 2 (**Pyk2**) (Fisslthaler et al., 2008; Viswambharan et al., 2017).

Despite the potential link to diabetes, the impact of **Pyk2** on rIPC-mediated remote organ protection in diabetes has not yet been investigated. This study addresses the hypothesis that endothelium-dependent cardioprotection mediated by rIPC is abolished in diabetes

What is already known

- Remote ischaemic preconditioning describes the protective effect of local ischaemia on a subsequent cardiac ischaemia.
- Diabetes is associated with endothelial dysfunction and loss of remote organ protection by ischaemic conditioning.

What does this study add

- Proline-rich tyrosine kinase 2 (Pyk2) inhibits eNOS activity and impairs cardioprotection by ischaemic preconditioning.
- Inhibition of Pyk2 restores eNOS activity, endothelial function and remote ischaemic cardioprotection in diabetes.

What is the clinical significance

- Pyk2 inhibition restores remote cardioprotection and attenuates infarct size after acute myocardial infarction in diabetes.
- Pyk2 may be a target to improve the outcomes in diabetes with acute myocardial infarction.

and that inhibition of Pyk2 could restore eNOS activity and endothelial function to limit infarct size and LV dysfunction following ischaemia and reperfusion.

2 | METHODS

The NZO mouse strain is an established and well-known polygenic model exhibiting the characteristic features of diabetes in humans, that is, obesity, insulin resistance, severe hyperglycaemia and disturbed glucose tolerance (Dreja et al., 2010; Jonas et al., 2022; Knebel et al., 2018; Rehman et al., 2021). Since only approximately 60% of adult male NZO mice develop a diabetic phenotype, we only investigated NZO mice presenting all of the characteristics of diabetes, including obesity, hyperinsulinaemia and hyperglycaemia, in our experiments. Mice not exhibiting these features were not used for analysis. Those NZO mice exhibiting the full pattern of diabetes were included for analysis and referred to as diabetic NZO mice.

To investigate the role of the vascular endothelium in transmitting signals for remote tissue protection after rIPC, we performed transfer experiments with plasma from diabetic and non-diabetic mice and humans subjected to rIPC or not. These experiments were followed by in vivo and ex vivo experiments showing that C57BL/6J (BL6) and New Zealand obese (NZO) mice exhibit endothelial dysfunction and loss of eNOS functional activity. Next, we analysed the impact of Pyk2 on eNOS-dependent remote tissue protection. The ability of Pyk2 inhibition to restore the endothelium-dependent effects of rIPC in mediating remote tissue protection was analysed.

2.1 | Materials

Unless otherwise specified, chemicals were purchased from Sigma–Aldrich Co. LLC (Deisenhofen, Germany). Materials for Western blotting were purchased from Life Technologies (Invitrogen, Darmstadt, Germany), Cell Signaling Technology (Massachusetts, EUA), DB Bioscience and Abcam (Cambridge, UK).

2.2 | Transfer experiments in humans and mice with and without diabetes

Five subjects with a history of cardiovascular diseases and diabetes (type 2 DM) and five age-matched subjects without diabetes were included. The exclusion criteria for both groups were chronic kidney disease (estimated glomerular filtration rate <30 $ml \cdot min^{-1}$), known liver disease, acute myocardial infarction, elevated C-reactive protein levels or elevated white blood cells numbers.

Human plasma samples were collected before and after rIPC was applied. All clinical investigations and transfer experiments were performed according to the study protocol approved by the ethics committee of the Heinrich-Heine University of Duesseldorf (ID2017034183–5903R) following the Declaration of Helsinki and institutional guidelines. Written informed consent was obtained from all participants.

Plasma dialysates were added to the perfusion solution of BL6 mouse hearts in a Langendorff apparatus. Briefly, changes in LV function were assessed by measuring LV-developed pressure, LVEDP and +dP/dt and −dP/dt. Cardioprotective effects were evaluated by measuring the infarct size (by triphenyltetrazolium chloride staining) after 30 min of ischaemia followed by 2 h of reperfusion (Figure S1).

Similarly, aortic rings were incubated with native and preconditioned plasma. The rings were consequently rinsed, and their function was tested in response to acetylcholine, phenylephrine (Phe) and sodium nitroprusside (SNP) according to our previously described protocol (Erkens et al., 2015).

2.3 | Animals

All experiments were performed with 15- to 18-week-old male New Zealand obese (NZO/HILtJ), C57BL/6J (BL6) and global eNOS knockout ($eNOS^{-/-}$) mice. NZO mice (Kluge et al., 2012) were obtained from the German Diabetes Center (Professor Dr. Al-Hasani, Germany). BL6 mice were purchased from the Jackson Laboratory (The Jackson Laboratory, Bar Harbor, ME, USA) or Janvier Labs (Janvier Labs, Le Genest-Saint-Isle, France). Global $eNOS^{-/-}$ mice on the C57BL/6J background were obtained from Professor Dr. Axel Gödecke, Heinrich Heine University of Düsseldorf, Düsseldorf, Germany (Gödecke et al., 1998). All mice received ad libitum drinking water and a standard rodent diet and were allowed to acclimate to the vivarium conditions for a minimum of 7 days, and they were housed on a 12/12 h light/dark cycle at the central animal research facility of Heinrich-Heine University, Düsseldorf, Germany. Animal studies are reported in compliance with the ARRIVE guidelines (Percie du Sert et al., 2020) and with the recommendations made by the *British Journal of Pharmacology* (Lilley et al., 2020). The mouse experiments were approved by the local animal ethics committee (AZ 84-02.04.2014. A432 and AZ 81-02.04.2020. A117, NRW, Germany) according to the European Convention for the Protection of Vertebrate Animals Used for Experimental and other Scientific Purposes (Council of Europe Treaty Series No. 123).

2.4 | Pyk2 inhibition

Pharmacological Pyk2 inhibition was achieved with PF-431396 hydrate (Sigma–Aldrich/Merck, Germany). PF-431396 is a known inhibitor of Pyk2 and focal adhesion kinase (FAK) kinases with $IC_{50} = 11$ and 1.5 nM, respectively. For the experiments, the inhibitor was diluted in a saline solution containing 2% dimethyl sulfoxide (DMSO) and administered at a concentration of 5 $\mu g \cdot g^{-1}$ of body

weight via intraperitoneal injection 15 min before the beginning of each protocol (Bibli et al., 2017). Control mice received vehicle (saline solution containing 2% DMSO).

2.5 | Remote ischaemic preconditioning

The rIPC protocol consisted of four cycles of ischaemic preconditioning (Figure S1). For this purpose, a vascular occluder (8 mm diameter, Harvard Apparatus, Harvard, Boston, MA, USA) was placed around the left hindlimb of anaesthetized mice (1.5%–2% isoflurane). The cuff was inflated (Druckkalibriergerät KAL 84, Halstrup Walcher, Kirchzarten, Germany) to a pressure of 200 mmHg for 5 min, leading to total occlusion of the artery. Subsequently, the occluder was deflated, allowing tissue reperfusion for 5 min. This protocol was repeated four times before further measurements were performed or procedures were implemented. In humans, ischaemia was induced with a blood pressure measuring cuff (Welch Allyn GmbH, Hechingen, DE). The cuff was placed on the upper lower arm and inflated to 250 mmHg (minimum of 50 mmHg above normal systolic blood pressure). The pressure was kept constant for 5 min. Consequently, the cuff was deflated, allowing reperfusion of the artery for 5 min. This procedure was repeated four times.

2.6 | Model of ischaemia–reperfusion and assessment of infarct size

The mice were randomly divided into the experimental groups shown in Figure S2. After adequate analgesia with buprenorphine (0.1 $mg \cdot kg^{-1}$), mice were intubated and anaesthetized with isoflurane (induction: 3% V/V; maintenance: 2% V/V) via the side port of a rodent ventilator. Regardless of the protocol used, mice in all groups were anaesthetized for the same duration. Heart rate was recorded by a PowerLab 4.0 electrocardiogram recorder (AD Instruments, UK). The respiratory rate (approximately 110–120 breaths min^{-1}) and body temperature (37.5°C) were kept constant throughout the experiment. The chest was opened, and local myocardial ischaemia was induced by occlusion of the left anterior descending coronary artery (Prolene suture 8.0) for 30 min. ST elevation on electrocardiogram confirmed the success of left anterior descending artery occlusion. Consequently, the left anterior descending coronary artery was reperfused, the chest was closed and the mice were subjected to 24 h of reperfusion (Erkens et al., 2018). Postoperative analgesia was achieved by s.c. buprenorphine (0.5 $mg \cdot kg^{-1}$ BW) injection every 8 h until the mouse was killed.

On the following day, infarct size was determined by triphenyl tetrazolium chloride staining, as described previously (Erkens et al., 2018). After adequate anaesthesia (100 $mg \cdot kg^{-1}$ BW ketamine and 10 $mg \cdot kg^{-1}$ BW xylazine, intraperitoneal injection) and anticoagulation with heparin (250 IU, intraperitoneal), hearts were excised and perfused with 0.9% NaCl. Excision of the hearts assured death of the mouse. The left anterior descending artery was occluded in the same location as before, and 1% Evans blue dye was injected into the aortic root to delineate the area at risk from the area not at risk. The hearts were frozen at −20°C for 60 min and serially sectioned into 1 mm slices; each slice was weighed and incubated in 1% triphenyltetrazolium chloride staining solution for 5 min at 37°C. The slices were photographed under a stereo microscope. The area at risk and non-ischaemic area were evaluated by computer-assisted planimetry (Diskus software, Hilgers Technisches Büro, Königswinter, Germany) by an observer blinded to the sample identities. The infarct size is expressed as the percentage of infarcted tissue area relative to the total area at risk.

2.7 | Ultrasound imaging measurements

High-resolution micro-ultrasound imaging-related parameters (LV geometry and function, flow-mediated dilation [FMD], pulse wave velocity) were measured using a Vevo 2100/3100 instrument (Fujifilm VisualSonics Inc., Toronto, Canada). The mice were kept in a stable cardiopulmonary state under isoflurane anaesthesia (1.5%–2%). Analysis of LV function (18–38 MHz transducer, Toronto, Canada) was performed as described previously (Erkens et al., 2015). Specifically, LV end-systolic volume (ESV) and end-diastolic volume (EDV), ejection fraction (EF), cardiac output (CO) and stroke volume (SV) were calculated in B-mode by identification of the maximal and minimal cross-sectional area using the software Vevo Lab 5.6.1 (Visual Sonics Inc.). These were normalized to the body surface area and body weight and reported as end-systolic volume index (ESVI), end-diastolic volume index (EDVI), cardiac index (CI) and stroke volume index (SVI). The body weight value used for normalization was measured prior to echocardiographic analyses.

Assessment of endothelial function in vivo by FMD was performed by a method previously described in our laboratory (Erkens et al., 2015) with some modifications. After isoflurane anaesthesia (1.5%–2%) and achieving a stable cardiopulmonary state (heart rate: 400–500 bpm, breathing rate: ∼100 breaths min^{-1}, body temperature: 37°C), a 30–70 MHz linear array Microscan transducer (Vevo 2100/3100, Visual Sonics Inc.) placed in a stereotactic holder was positioned to visualize the arteria iliaca externa. A vascular cuff (8 mm diameter, Harvard Apparatus, Harvard, Boston, MA, USA) was placed on the same lower extremity of the mouse, distal to the transducer. After recording baseline images, the blood flow in the artery was ceased by inflating the occluder to 250 mmHg (Druckkalibriergerät KAL 84, Halstrup Walcher, Kirchzarten, Germany), and the pressure was kept constant for 5 min. The occluder was then deflated, and several recordings of the vessel were performed during subsequent vasodilation. Based on the images recorded during occlusion and reperfusion, vessel diameter (%) changes at specific time-points were calculated as follows: $(\text{diameter}_{\text{time-point}}/\text{diameter}_{\text{baseline}}) \times 100$. The difference in maximum dilation was calculated from the vessel diameter values obtained after cuff deflation as follows:

$$\Delta Max(\%) = \frac{diameter(max) - diameter(BL)}{diameter(BL)} \times 100.$$

Vascular stiffness was assessed by measuring the pulse wave velocity by a method previously described by us (Erkens et al., 2015). Briefly, the distance (ΔD) between the common carotid artery and the external iliac artery was divided by the time (ΔT) needed for the blood to travel between the two arteries, which was measured from B-mode, M-mode and PV-Doppler images.

2.8 | Blood glucose and plasma insulin level measurement

Glucose tolerance measurements were performed in mice following 8 h of fasting. After baseline measurement, the mice received glucose (1 g·kg^{-1} BW) intraperitoneally for the glucose tolerance test. Consecutive measurements of blood glucose (Contour XT; Bayer Health Care, Leverkusen, Germany) and plasma insulin (insulin mouse ultrasensitive ELISA; DRG Instruments, Marburg, Germany) levels were performed 15, 30, 60, 120 and 240 min after glucose administration by extracting small amounts of blood from the tail vein.

2.9 | Aortic ring bioassay

Aortae were isolated, the adjacent fat tissue was removed and the aortae were cut into 2–3 mm long rings. The aortic rings were mounted on 300 μm wires in organ baths (Graz Glass Tissue Bath, 2 ml, Hugo Sachs Elektronik, March, DE) perfused with Krebs–Henseleit solution (KH buffer: NaCl [118 mM], KCl [4.7 mM], $MgSO_4$ [0.8 mM], $NaHCO_3$ [25 mM], KH_2PO_4 [1.2 mM], glucose [10 mM] and $CaCl_2$ [2.5 mM]) equilibrated with a mixture of 95% O_2 and 5% CO_2 and calibrated for 60 min. The tension between the wires was measured by a transducer (F30 Force Transducer Type 372, Hugo Sachs Elektronik, March, Germany), amplified by a PowerLab 8/30 (ADInstruments–Europe Head Office, Oxford, UK) and recorded with LabChart (ADInstruments). The maximum contraction was determined by applying KCl (80 mM) to the baths. EC function was assessed by measuring the response to cumulative doses of acetylcholine (Ach, 0.1 nM–10 μM) or carbachol (0.1 nM–10 μM) after precontraction with a bolus of the **α_1-adrenoceptor** agonist phenylephrine (Phe) equal to the half-maximal effective concentration (EC_{50}). The function of the VSMCs was assessed as response to cumulative doses of sodium nitroprusside (SNP; 0.01 nM–10 μM) and Phe (0.1 nM–10 μM).

Transfer experiments with the plasma of mice and humans with diabetes, with or without rIPC, were performed according to a standard organ bath protocol with some modifications. Blood was obtained from mice via cardiac puncture and from humans via venous puncture before and after rIPC. Plasma was separated after centrifugation in fully heparinized tubes. Aortic rings were incubated with a plasma/KH solution and continuously performed with a mixture of 95% O_2 and 5% CO_2. In some experiments, endothelial function was tested in response to cumulative doses of carbachol (0.1 nM–10 μM) to exclude any effect of acetylcholine degradation by cholinesterase. Natural product studies are reported in compliance with the recommendations made by the *British Journal of Pharmacology* (Izzo et al., 2020).

2.10 | Assessment of murine cardiac function after treatment with plasma from humans

Hybrid transfer experiments involved the perfusion of murine hearts (BL6 mice) with plasma from preconditioned healthy and diabetic individuals. These experiments followed a previously reported protocol with several modifications. Human plasma samples (4 ml) obtained at baseline and after rIPC were placed in 12 to 14 kDa dialysis tubes (SpectraPor, Spectrum Europe B.V., Breda, the Netherlands) and dialyzed for 24 h at 4°C in a 20-fold volume of modified Krebs–Henseleit buffer. The dialysates were then oxygenated and equilibrated to 37°C before use.

After adequate anaesthesia with ketamine (100 mg·kg^{-1} BW, intraperitoneal injection) and xylazine (10 mg·kg^{-1} BW, intraperitoneal injection) and anticoagulation with heparin (250 IU, intraperitoneal), the hearts of BL6 mice were explanted, mice were killed and the ascending aorta was cannulated and connected to a Langendorff apparatus (Hugo Sachs Electronics, March-Hugstetten, Germany). The equilibration phase started with retrograde perfusion with modified Krebs–Henseleit buffer (NaCl [118 mM], KCl [4.7 mM], $MgSO_4$ [0.8 mM], $NaHCO_3$ [25 mM], KH_2PO_4 [1.2 mM], glucose [5 mM], pyruvic acid [1.9 mM] and $CaCl_2$ [2.5 mM]) at a constant pressure of 100 mmHg.

Cardiac and coronary endothelial parameters were evaluated ex vivo by a Langendorff apparatus as previously described (Flögel et al., 1999). A water-filled balloon connected to a pressure transducer was inserted through the mitral valve into the LV for the recording of isovolumetric LV developed pressure, its positive and negative first derivate (+dP/dt and −dP/dt) and the LV end-diastolic pressure (LVEDP). Consequently, hearts were subjected to 20 s of global zero flow ischaemia to test the coronary reserve, followed by a 5-min recovery. Readouts of the hybrid transfer analyses were the derivates of the LVEDP (dP/dT_{max} as measures of contractility, dP/dT_{min} as measures of relaxation), the LVEDP and infarct sizes per left ventricle (assessed by triphenyl tetrazolium chloride staining) following 30 min of global ischaemia and subsequent 2 h of reperfusion. Hearts were excluded from the analysis if they met one of the following exclusion criteria after the 5-min recovery phase: (I) coronary flow > 4 ml·min^{-1}, (II) LV developed pressure < 50 mmHg or (III) a coronary flow reserve revealed by transient ischaemia <70% of the baseline flow.

2.11 | Determination of NO metabolite levels in plasma

NO metabolite levels have been analysed in plasma from mice and humans. The mice were anaesthetized with isoflurane (1.5%–2%).

Blood was collected by cardiac puncture (murine experiments) or venous puncture (human experiments) and placed in a tube containing 100 µl of N-ethylmaleimide/EDTA/PBS (100 mmol·L^{-1} N-ethylmaleimide and 5 µl of 0.5 mmol·L^{-1} EDTA) solution. Subsequently, the blood solution was centrifuged at 3000 × *g* for 2 min at 4°C. The plasma and red blood cells (RBCs) were separated, immediately frozen in liquid nitrogen and stored at −80°C until further analysis.

At the time of measurement, plasma samples were thawed on ice, and nitrite concentrations were quantified by a chemiluminescence detector (CLD 88 e, Eco Physics GmbH, Munich, Germany) as previously described (Rassaf et al., 2014). Plasma nitrate concentrations were measured by high-performance liquid chromatography with an ENO-30 instrument (AMUZA INC, San Diego, USA) following the manufacturer's instructions. Acquired data were analysed with eDAQ Powerchrome software (eDAQ, Warsaw, Poland) (Rassaf et al., 2014).

2.12 | Assessment of systemic haemodynamics

Haemodynamic parameters were assessed by the invasive close-chest method described previously (Erkens et al., 2015). The method uses a 1.4 F Millar pressure conductance catheter (SPR-839, Millar Instrument, Houston, TX, USA) inserted into the LV through the right carotid artery. A Millar Box was used to record the pressure, LV developed pressure, rate of pressure development (dP/dt_{max}) and rate of pressure decrease (dP/dt_{min}). Acquired data were analysed by LabChart 7 (AD Instruments, Oxford, UK).

2.13 | Organ harvesting and molecular analysis

Mice were anaesthetized with 100 mg·kg^{-1} ketamine (Ketanest®) and 10 mg·kg^{-1} xylazine (Rompun®) via i.p. injection. Heparin (25,000 E.I. B.Braun, Melsungen, Germany) was administered intraperitoneally 5 min before blood collection. Blood samples were collected by cardiac puncture and immediately centrifuged at 800 × *g* for 10 min at 4°C. Plasma samples were collected, frozen in liquid nitrogen and stored in a −80 freezer until further analysis. After systemic perfusion with cold phosphate-buffered solution without calcium and magnesium (pH 7.4) (Sigma Aldrich), organs were collected, immediately placed into tubes, frozen in liquid nitrogen and stored in a −80 freezer until further analysis. Death was confirmed by heart explantation.

2.14 | Western blotting

Whole hearts were collected and the samples were lysed with RIPA buffer (1% NP40, 0.1% SDS, 0.5% sodium deoxycholate in PBS) containing a mixture of protease and phosphatase inhibitors (Donato et al., 2007) and homogenized with a Tissue Ruptor instrument (Qiagen, Hilden, Germany). Afterwards, the samples were placed in an ultrasonic bath at 4°C for 10 min. Afterwards, the samples were centrifuged at 13,300 × *g* for 15 min at 4°C, and the supernatant was collected.

Total protein concentrations were determined by a Bio-Rad DC Protein Assay (Bio-Rad Laboratories, California, USA). For immunoblotting, 75–100 µg of protein was loaded on NuPAGE™ 4%–12% Bis-Tris Precast gels following the manufacturer's instructions. After electrophoresis, the proteins were transferred onto Hybond P 0.2 nitrocellulose membranes (Amersham Biosciences, Munich, Germany). The membranes were blocked for 1 h with 2% Amersham ECL Prime Blocking Reagent in T-TBS (10 mM Tris, 100 mM NaCl, 0.1%Tween) followed by overnight incubation at 4°C with one of the following: an anti-eNOS antibody (1:250; custom made from #624086) an anti-phospho (Ser1177)-eNOS antibody (1:500; #9571, Cell Signaling Technology, Cambridge, UK, RRID: RRID: AB_329837), an anti-phospho (Tyr402)-Pyk2 antibody (1:1000; #3291, Cell Signaling Technology, Cambridge, UK, RRID: AB_2300530), an anti-Pyk2 antibody (1:1000; #3292, Cell Signaling Technology, Cambridge, UK, RRID: AB_2174097) and an anti-GAPDH antibody (1:5000 Abcam, Cambridge, UK). The primary antibodies were diluted in T-TBS 5% BSA 0.1% Tween. After washing, the membranes were incubated with HRP-conjugated or antibodies (1:5000; BD Biosciences). For p (Tyr656)-eNOS, heart samples were pulverized on dry ice for immunoprecipitation and lysed in lysis buffer. For precipitation, 2 mg of protein lysate was incubated overnight with an anti-NOS III antibody (BD Bioscience 610297; AB_397691; 2 µg·mg^{-1} protein lysate). Afterwards, agarose immunoprecipitation was performed following the manufacturer's instructions. After elution, 25 µl of the sample was loaded on 8% SDS gels, and standard immunoblotting was performed. The membranes were incubated overnight with an anti-p (Tyr656)-eNOS antibody (custom-made by Eurogentec, diluted 1:500 in Rotiblock). For all Western blot analyses, the bands were visualized by chemiluminescence with Western Blotting Detection Reagent (GE Healthcare Amersham™ ECL Select™) with a Chemidoc imager (Bio-Rad California, USA). Band intensity quantification was performed using ImageJ software. The immuno-related procedures used comply with the recommendations made by the *British Journal of Pharmacology* (Alexander et al., 2018).

2.15 | Data and statistical analysis

If not otherwise mentioned, the results are displayed as the mean ± standard error of the mean (SEM). Statistical analyses were carried out by unpaired or paired t test for comparisons of two groups or by one-way or two-way analysis of variance (Rizvi et al., 2021), as appropriate, followed by Tukey or Šídák's post hoc test for comparisons of more than two groups or treatments. Normal distribution was tested through the D'Agostino-Pearson test. $P < 0.05$ was considered to indicate statistical significance. Post-hoc tests were run only if F achieved $P<0.05$ and there was no significant variance inhomogeneity. Statistical analysis was performed using GraphPad Prism 9 for Windows (GraphPad Software, San Diego, CA, USA). The data and statistical analysis comply with the recommendations of the *British Journal of Pharmacology* on experimental design and analysis in pharmacology (Curtis et al., 2022).

2.16 | Nomenclature of targets and ligands

Key protein targets and ligands in this article are hyperlinked to corresponding entries in http://www.guidetopharmacology.org, and are permanently archived in the Concise Guide to PHARMACOLOGY 2023/24 (Alexander, Christopoulos et al., 2023; Alexander, Fabbro et al., 2023).

3 | RESULTS

3.1 | The plasma from humans and mice with diabetes lacks signals for transmitting remote tissue protection

To test the hypothesis that rIPC induces the release of circulating messengers in the plasma to promote remote tissue protection, plasma was obtained from humans with or without type 2 diabetes mellitus (see Table S1 for full demographic data) after repetitive limb ischaemia (for protocol see Figure S1). Preconditioned plasma was analysed for nitrite levels and was added to the perfusate of a Langendorff-perfused heart or to an organ bath to assess endothelial function in isolated aortic rings (Figure 1a). The addition of preconditioned plasma from humans without diabetes to the perfusate of isolated hearts resulted in improved LV function and reduced infarct size after global ischaemia (Figure 1b). That was not the case when hearts were perfused with preconditioned plasma from humans with diabetes. rIPC led to a significant increase in plasma nitrite levels in healthy but not in diabetic humans (Figure 1c, Table S2 for full demographic data). Similarly, the acetylcholine-induced nitric oxide-mediated relaxation of aortic rings from BL6 mice was clearly greater in samples exposed to plasma from nondiabetic humans than to plasma before rIPC (Figure 1d). Responses to acetylcholine were however comparable in aortic rings exposed to plasma obtained from humans with type 2 diabetes mellitus independent of whether the rIPC protocol had been performed or not (Figure 1d). There was no effect of plasma from humans with or without diabetes on the vasoconstrictor response to Phe or the relaxation induced by SNP (Figure S3A). These experiments indicate that in non-diabetic humans, rIPC induces the release of one or more circulating messengers that are stable enough to be transferred to in vitro models. Since diabetes is associated with endothelial dysfunction, it is tempting to suggest that the endothelium is the source of these protective agent(s).

Next, we determined whether preconditioned murine plasma could have similar effects and added plasma from non-conditioned and preconditioned BL6 or diabetic NZO mice to aortic rings from BL6 mice. As was the case with the human samples, plasma from mice that underwent the rIPC protocol improved responsiveness to acetylcholine versus responses recorded in the presence of plasma from mice that did not experience preconditioning (Figure 1d). Plasma from diabetic NZO mice subjected to rIPC did not have any beneficial impact over plasma from mice that did not experience preconditioning.

Importantly, giving a Pyk2 inhibitor to diabetic mice prior to rIPC did improve endothelium-dependent relaxation to acetylcholine. The latter effects were endothelium-dependent as the Pyk2 inhibitor did not alter vascular responses to either phenylephrine or sodium nitroprusside (Figure S3B). Collectively, these results hint that the inhibition of Pyk2 improves acetylcholine-induced relaxation in vessels from diabetic mice by enhancing eNOS activity.

3.2 | Pyk2 inhibits eNOS activity in diabetic NZO mice

Diabetic NZO mice displayed all key features of diabetes: (i) higher fasting glucose and insulin levels (Figure 2a), (ii) impaired glucose tolerance, (iii) insulin release in response to glucose (Figure 2b) and (iv) obesity with a heart weight to body weight ratio comparable to that of BL6 mice (Figure 2c).

Left ventricular (LV) functional parameters such as the stroke volume index (SVI), the cardiac index (CI) and ejection-fraction (EF) were comparable between diabetic NZO and BL6 mice (Table S2) at baseline. To link diabetes with Pyk2, we assessed its expression and phosphorylation (on Tyr402) as well as the expression and phosphorylation of eNOS on Ser1177 and Tyr656 in non-diabetic BL6 mice and diabetic NZO mice. The total Pyk2 abundance was lower, and the level of Pyk2 phosphorylation was significantly increased in diabetic NZO mice versus BL6 mice (Figure 2d). In the same samples, eNOS phosphorylation on Ser1177 was slightly decreased (Figure 2e). The tyrosine phosphorylation of eNOS on Tyr656 was then studied on eNOS immunoprecipitated from murine hearts and was found to be increased in the diabetic group (Figure 2f; all areas corresponding to the dots are shown in Figure S4). Intraperitoneal injection of the Pyk2 inhibitor prevented the tyrosine phosphorylation of eNOS in diabetic NZO mice but not in nondiabetic BL6 mice.

3.3 | Inhibition of Pyk2 restores endothelium-dependent relaxation and eNOS activity in diabetic mice

Next, endothelium-dependent vasodilation was assessed in vivo (flow-mediated dilation, FMD) and ex vivo (organ bath). FMD was detected in BL6 mice but abolished in diabetic NZO mice (Figure 3a); The degree of endothelial dysfunction in diabetic NZO mice was similar to that recorded in eNOS$^{-/-}$ mice (Figure S6A) and BL6 mice treated with the eNOS inhibitor S-ethylisothiourea (Figure S6A,B) (Erkens et al., 2015). Importantly, treating the diabetic mice with the Pyk2 inhibitor PF-431396 largely restored FMD to levels seen in BL6 mice (Figure 3a). Pyk2 inhibition also significantly increased the acetylcholine-induced, endothelium-dependent relaxation of aortic rings from diabetic NZO mice (Figure 3b). In contrast, the inhibitor did not alter endothelial function in non-diabetic BL6 mice (Figure S5A) or vascular smooth muscle cell responsiveness to either phenylephrine

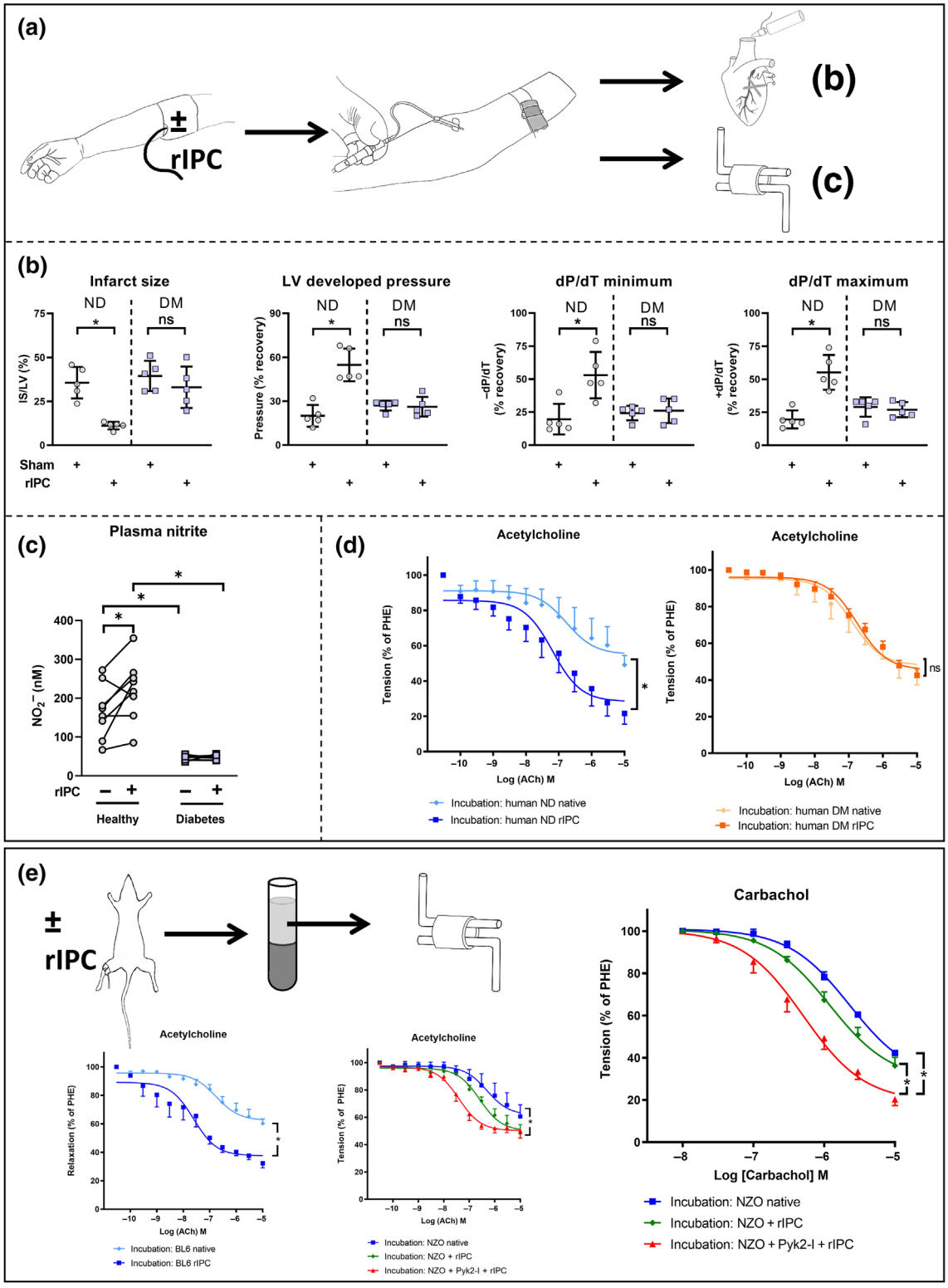

FIGURE 1 Legend on next page.

FIGURE 1 Remote tissue protection (rIPC) is abolished in humans and mice with diabetes. (a) Remote ischaemic conditioning by repeated occlusion/reperfusion was performed in the forearms of humans with type 2 diabetes mellitus (DM) or without diabetes (non diabetic: ND). After blood collection, plasma was transferred either to Langendorff heart preparations prior to global ischaemia, or for NO_2^- measurements, or to aortic rings from BL6 mice. (b) Plasma from humans without diabetes who underwent rIPC, but not plasma from humans with diabetes who underwent rIPC, decreased the infarct size (IS) per left-ventricle (LV) and increased LV developed pressure, cardiac relaxation (dP/dTmin) and contractility (dP/dTmax). Statistical significance was analysed by paired *t* tests. $n_{ND} = 5$, $n_{DM} = 5$; $^{ns}P > 0.05$, $^{*}P < 0.05$. (c) Significant increase in NO_2^- levels after the rIPC-manoeuvre in plasma from non-diabetic but not in plasma from diabetic humans. Statistical significance was analysed by two-way ANOVA followed by Šídák's multiple comparisons test. $n_{ND} = 8$, $n_{DM} = 7$; $^{*}P < 0.05$. (d) The endothelium-dependent relaxation response in isolated rings was increased by plasma from humans without diabetes who underwent rIPC but not by plasma from humans with diabetes who underwent rIPC. "native" reffers to non-conditioned plasma. Statistical significance was analysed by repeated-measurements two-way ANOVA. $n_{ND} = 5$, $n_{DM} = 5$. *P*-value for interaction is displayed in the graphics. $^{ns}P > 0.05$, $^{**}P < 0.01$. (e) Systemic Pyk2 inhibition (Pky2-I) restored the rIPC-associated release of circulating signals into plasma for remote tissue protection. BL6 or diabetic NZO mice with or without Pyk2 inhibition were subjected to rIPC. Blood samples were drawn, and plasma was transferred to aortic rings of Bl6 mice in organ baths. Conditioned plasma from control mice improved endothelial function in aortic rings, while conditioned plasma from diabetic NZO mice subjected to rIPC showed no effect. Plasma from diabetic NZO mice subjected to rIPC in the presence of a Pyk2(Pyk2-I) inhibitor improved endothelial function in aortic rings. "native" reffers to non-conditioned plasma. Statistical significance was analysed by repeated-measurement two-way ANOVA for two groups and displayed as *P*-value for interaction. For three groups, statistical significance was assessed by repeated-measurements two-way ANOVA with Tukey's multiple comparisons test, and the difference between the groups was shown by the *P*-value in the multiple comparison test. For experiments with acetylcholine: $n_{BL6\ +\ native} = 5$, $n_{BL6\ +\ rIPC} = 6$; $n_{NZO\ +\ native} = 5$, $n_{NZO\ +\ rIPC} = 5$, $n_{NZO\ +\ Pyk2\text{-}I.\ +\ rIPC} = 5$. For experiments with carbachol: $n_{NZO\ +\ native} = 5$, $n_{NZO\ +\ rIPC} = 5$, $n_{NZO\ +\ Pyk2\text{-}I.\ +\ rIPC} = 8$. $^{*}P < 0.05$.

or sodium nitroprusside (Figure S5B,C). Additionally, the vehicle control DMSO did not have any effect in any of the experiments performed.

Endothelial dysfunction has been linked to arterial stiffness (Schremmer et al., 2023), and consistent with the impaired endothelial function in diabetic mice, the elasticity of conductance of arteries in diabetic NZO mice was impaired while pulse wave velocity was increased (Figure 3c). The pulse wave velocity in diabetic NZO mice was comparable to that in $eNOS^{-/-}$ mice, indicating the importance of functional eNOS for preserving arterial vessel elasticity. Plasma levels of nitrite (NO_2^-) reflected the diabetic status of the animals i.e. were lower in the NZO group. The rIPC protocol stimulated eNOS in non-diabetic mice to increase NO_2^- but again hat no impact on circulating NO_2^- in diabetic NZO mice (Figure 3d). Pyk2 inhibition, however, restored the effect of rIPC so that nitrite levels were comparable to those in BL6 mice subjected to rIPC (Figure 3d).

The impact of diabetes on systemic haemodynamics was evaluated using a Millar catheter. This approach revealed that diabetic NZO mice displayed a significantly higher systolic (Figure 3e) and mean arterial (Figure 3f) pressure but no change in diastolic pressure (Figure 3g) and an associated increase in total peripheral resistance (Figure 3h). The Pyk2 inhibitor reversed the increase in arterial pressure in diabetic NZO mice (Figure 3e–h, Table S2).

3.4 | Endothelium-dependent remote cardioprotection is impaired in diabetic NZO mice and restored by Pyk2 inhibition

Next, we assessed the impact of diabetes with and without Pyk2 inhibition on rIPC-mediated cardioprotection in diabetic and nondiabetic mice after ischaemia followed by reperfusion (Figure 4a).

Infarct sizes were larger following ischaemia and reperfusion in diabetic NZO than in BL6 mice (Figure 4b), and left ventricular function was more significantly impaired (Figure 4c). In non-diabetic mice, the rIPC protocol significantly reduced the infarct size and improved LV function after ischaemia and reperfusion, while the rIPC protocol was ineffective in animals with diabetes. rIPC increased circulating NO_2^- levels indicating the activation of eNOS, and, although supplementation with nitrite (48 nM in 50 µl) did not further reduce infarct size in BL6 mice that received rIPC, rIPC significantly reduced infarct size and improved LV function in diabetic NZO mice. Conversely, scavenging circulating NO using 2-4-carboxyphenyl-4,-4,5,5-tetramethylimidazoline-1-oxyl-3-oxide (cPTIO) markedly increased infarct sizes in BL6 mouse hearts. The administration of cPTIO in combination with rIPC largely neutralized the NO-dependent cardioprotective effects observed in non-diabetic mice. NO scavenging did not affect the infarct size or LV function parameters in diabetic NZO mice (Figure 4b,c and Table 1), presumably because the endothelium was already clearly dysfunctional. The corresponding areas at risk for all treatment groups are shown in Figure S7A.

To examine the consequences of targeting Pyk2, experiments were repeated using PF-431396 (Figure 5a and Table 2). We observed that the Pyk2 inhibitor restored rIPC-induced cardioprotection in diabetic NZO mice; that is, it reduced infarct size and improved LV function (Figures 5b,c and S7B). These protective effects were abolished by the NO scavenger cPTIO, suggesting that eNOS-derived NO underlies the cardioprotective effects of rIPC. Several theories have been proposed to account for the phenomenon of rIPC, including the activation of neuronal pathways (Heusch, 2020). To address the input from femoral nerves, non-diabetic BL6 mice and diabetic NZO mice were subjected to femoral nerve dissection prior to rIPC (Figure S8A, area at risk in Figure S8B). The dissection protocol prevented the rIPC-mediated decrease in infarct size in Bl6 mice, indicating that both endothelium-dependent signalling and neuronal pathways contribute to the remote tissue-protective effect of rIPC in healthy mice. This effect was not observed in diabetic NZO mice. The Pyk2 inhibitor restores remote cardioprotection, independently of prior nerve

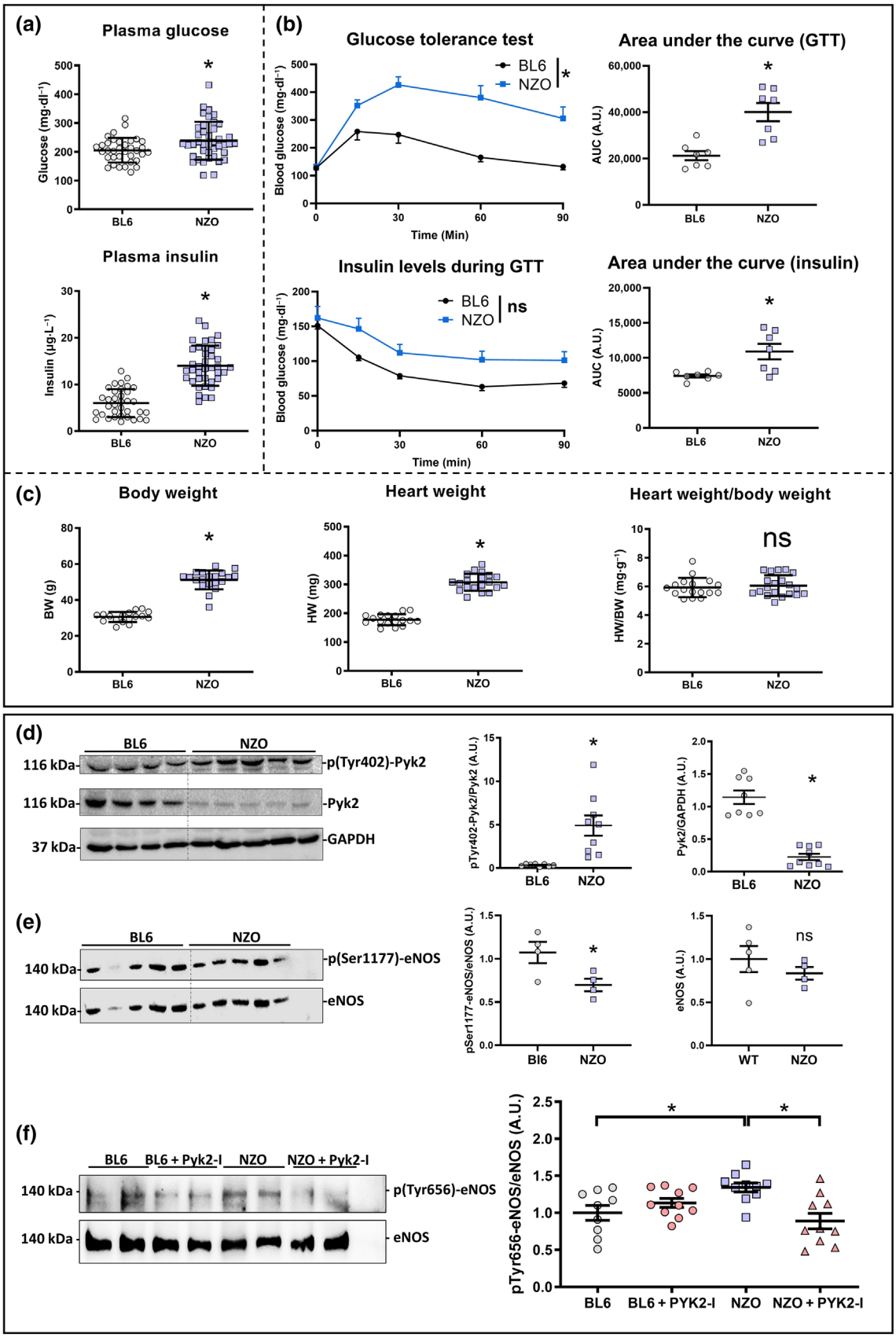

FIGURE 2 Legend on next page.

FIGURE 2 Metabolic and molecular alterations in diabetic NZO mice. (a) Blood glucose and plasma insulin levels of BL6 and diabetic NZO mice. Statistical significance was analysed by unpaired *t* tests. $n_{BL6} = 35$, $n_{NZO} = 39$. $^{*}P < 0.05$. (b) Glucose tolerance test (GTT) results and area under the curve (AUC) of blood glucose levels during the glucose tolerance test. Plasma insulin levels during the glucose tolerance test and the corresponding AUC. Statistical significance was analysed by repeated-measurements two-way ANOVA for glucose/insulin values over time and by unpaired *t* tests for the corresponding areas under the curve. $n_{BL6} = 7$, $n_{NZO} = 7$. $^{ns}P > 0.05$, $^{*}P < 0.05$. (c) Body weight, heart weight and the heart weight/body weight (HW/BW) ratio of BL6 and diabetic NZO mice. Statistical significance was analysed by unpaired *t* tests. $n_{BL6} = 17$, $n_{NZO} = 20$. $^{ns}P > 0.05$, $^{*}P < 0.05$. (d) Representative western blots and densitometric analysis of p (Tyr402)-Pyk2 and total Pyk2 levels in cardiac tissue from BL6 and diabetic NZO mice. Pyk2-I: Pyk2 inhibition. Statistical significance was analysed by unpaired *t* tests. $n_{BL6} = 8$, $n_{NZO} = 9$. $^{*}P < 0.05$. (e) Representative western blots and densitometric analysis of the levels of p (Ser1177)-eNOS (stimulatory site) and total eNOS in cardiac tissue from BL6 and diabetic NZO mice. Statistical significance was analysed by unpaired *t* tests. $n_{BL6} = 5$, $n_{NZO} = 5$. $^{ns}P > 0.05$, $^{*}P < 0.05$. (f) Representative western blots and densitometric analysis of the levels of p (Tyr656)-eNOS (inhibitory site) and total eNOS in cardiac tissue from BL6 and diabetic NZO mice. Statistical significance was analysed by ordinary one-way ANOVA followed by Tukey's multiple comparisons test. $n_{BL6} = 9$, $n_{BL6 + Pyk2\text{-}I.} = 10$, $n_{NZO} = 10$, $n_{NZO + Pyk2\text{-}I.} = 10$. $^{*}P < 0.05$.

dissection. Apparently, neuronal signalling pathways are disturbed in diabetes, thus further emphasizing the importance of Pyk2 in the modulation of eNOS-dependent remote tissue protection.

4 | DISCUSSION

The results of the present study highlight the role of Pyk2 in modulating endothelial function and remote tissue protection by rIPC and, thus, the potential of targeting Pyk2 as a novel approach to re-establish both endothelial cell function and the protective effect of rIPC in diabetes.

We showed that (1) in diabetic NZO mice, metabolic dysregulation was associated with severely impaired endothelium-dependent aortic ring relaxation in response to acetylcholine, singular or repetitive limb ischaemia/reperfusion, reduced circulating NO bioactivity, increased arterial stiffness and elevated blood pressure; (2) in nondiabetic humans and mice, repetitive limb ischaemia induced eNOS activation, flow-dependent dilation and the release of NO as a plasma-transmitted signal for tissue protection. These protective signals were absent in the plasma of humans with diabetes and of diabetic NZO mice. (3) Pyk2 was strongly activated in diabetic mice, increasing the phosphorylation of eNOS on Tyr656, associated with severe endothelial dysfunction and loss of tissue protection. (4) The inhibition of Pyk2 restored eNOS function by dephosphorylation of Tyr656, resulting in the restoration of endothelial function and the cardioprotective effects of rIPC in diabetic NZO mice, which limited the infarct size. (5) Scavenging of NO using cPTIO abolished the cardioprotective effect of Pyk2 inhibition in diabetic NZO mice, while the administration of nitrite restored it. All of this evidence taken together supports the notion that the generation of eNOS-derived NO is an absolute prerequisite for remote tissue protection by rIPC and that the inhibition of Pyk2 restores eNOS activity, the missing link in diabetic conditions.

4.1 | eNOS and Pyk2 regulation

The NZO mouse strain is an established murine model of metabolic syndrome and diabetes (Haskell et al., 2002). Male mice develop all symptoms of the human metabolic syndrome and type 2 diabetes mellitus, including early-onset obesity, insulin resistance, hyperlipidaemia, hypercholesterolaemia, hypertension and ultimately β-cell failure (Bielschowsky & Bielschowsky, 1956; Ortlepp et al., 2000). Unlike monogenic models, diet and duration of hyperglycaemia significantly influence the development of diabetes in NZO mice, highlighting their utility for translational research (Dreja et al., 2010). Conversely, BL6 mice remain resistant to type 2 diabetes due to unidentified genetic factors that prevent beta cell failure and hyperinsulinemia, despite potential obesity and leptin signalling deficiencies (Joost & Schurmann, 2014).

Downstream signalling by insulin receptor activation activates Akt and finally eNOS, which is part of the canonical insulin signalling pathway. In tonic insulin receptor activation, the inhibition of eNOS by Tyr657 phosphorylation exceeds the effect of the canonical pathway, resulting in endothelial dysfunction. The subsequent effects are a decrease in systemic haemodynamics and large arterial stiffness as observed in diabetic NZO mice. Indeed, diabetic NZO mice display isolated systolic hypertension and increased total peripheral resistance and pulse wave velocity, indicating an imbalance in large arterial compliance. In diabetes, the balance between the anti-atherogenic metabolic insulin-receptor pathway and the mitogenic insulin-receptor pathway is disturbed in favour of the mitogenic pathway. As a consequence, insulin-induced eNOS activation is impaired. In addition, higher levels of oxidative stress might further enhance Pyk2 activity (Frank & Eguchi, 2003). Indeed, sustained stimulation of insulin receptors decreases cyclic guanosine monophosphate (cGMP) levels and NO-dependent relaxation (Fleming et al., 2003; Kolb et al., 2020; Randriamboavonjy et al., 2004). Of note, the mechanism underlying the regulation of eNOS activity is complex, and several regulatory phosphorylation events are responsible for eNOS activation/inhibition. In this manner, the phosphatase and tensin homologue (**PTEN**), a known inhibitor of Akt signalling (Mocanu & Yellon, 2007), can exhibit functional dysregulation in diabetes (Penna et al., 2020). Insulin has been previously reported to induce Pyk2-mediated inhibitory phosphorylation of eNOS at Tyr657 within the FMN binding domain to prevent the transfer of electrons and subsequently reducing the ability of eNOS to generate NO (Fisslthaler et al., 2008; Siragusa & Fleming, 2016; Viswambharan et al., 2017). Proatherogenic factors associated with diabetes, such as oxidative stress (Tai et al., 2002),

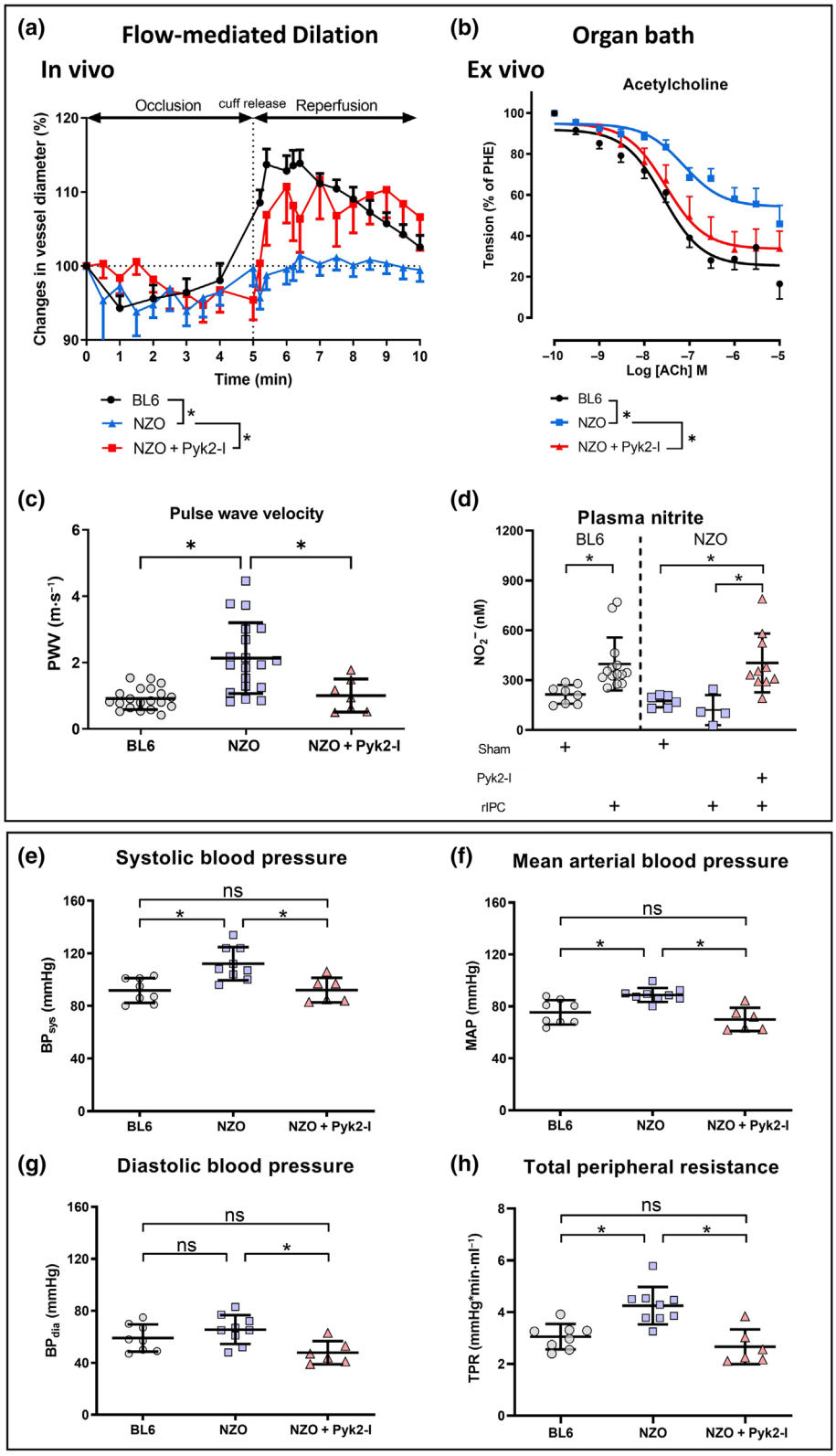

FIGURE 3 Legend on next page.

FIGURE 3 Diabetic NZO mice exhibit endothelial dysfunction and hypertension due to reduced NO bioavailability, which can be alleviated by Pyk2 inhibition (Pyk2-I). (a) Endothelial function assessed in vivo by noninvasive measurement of flow-mediated dilation (FMD). Intraperitoneal injection of a Pyk2 inhibitor (Pyk2-I) 15 min before examination rescued endothelial function in diabetic NZO mice. Compared were the maximum diameter changes from baseline between the groups. Statistical significance was analysed by ordinary one-way ANOVA followed by Tukey's multiple comparisons test. $n_{BL6} = 21$, $n_{NZO} = 23$, $n_{NZO + Pyk2\text{-}I.} = 14$. $^{*}P < 0.05$. (b) Organ bath experiments revealed a significant improvement in endothelial function in response to acetylcholine after Pyk2 inhibition (Pyk2-I) in diabetic NZO mice. Statistical significance was analysed by repeated-measurement two-way ANOVA with Tukey's multiple comparisons test and the difference between the groups were shown by the *P*-value in the multiple comparison test. $n_{BL6} = 13$, $n_{NZO} = 11$, $n_{NZO + Pyk2\text{-}I.} = 10$. $^{*}P < 0.05$. (c) Pyk2 inhibition normalizes the pulse-wave velocity in diabetic NZO mice. Statistical significance was analysed by ordinary one-way ANOVA followed by Tukey's multiple comparisons test. $n_{BL6} = 20$, $n_{NZO} = 19$, $n_{NZO + Pyk2\text{-}I.} = 7$. $^{*}P < 0.05$. (d) Increased plasma nitrite levels after Pyk2 inhibition indicate reactivation of eNOS functional capacity after shear-mediated activation by remote ischaemic preconditioning (rIPC). Statistical significance was analysed by unpaired *t* test between BL6 mice groups and by ordinary one-way ANOVA followed by Tukey's multiple comparisons test for diabetic NZO mice groups. $n_{BL6} = 8$, $n_{BL6 + rIPC} = 14$, $n_{NZO} = 6$, $n_{NZO + Pyk2\text{-}I.} = 6$, $n_{NZO + Pyk2\text{-}I. + rIPC} = 10$. $^{*}P < 0.05$. (e) Systolic pressure, (f) mean arterial blood pressure (MAP), (g) diastolic blood pressure and (h) total peripheral resistance (TPR) were increased in diabetic NZO mice compared to BL6 mice. Systemic inhibition of Pyk2 normalized blood pressure and vascular resistance in diabetic NZO mice compared to BL6 mice. (e–h) Statistical significance was analysed by ordinary one-way ANOVA followed by Tukey's multiple comparisons test. $n_{BL6} = 8$, $n_{NZO} = 9$, $n_{NZO + Pyk2\text{-}I.} = 6$. $^{ns}P > 0.05$, $^{*}P < 0.05$.

angiotensin II (Yin et al., 2003), atherosclerosis (Siragusa et al., 2019) and proteins of the mitogen-activated protein kinase (MAPK) family (Murphy et al., 2019) can elicit the activation of Pyk2. Within this study, we were able to demonstrate, that the activation of Pyk2 increases eNOS phosphorylation on Tyr656 and decreases the generation of NO in a model of diabetes. The tyrosine phosphorylation of eNOS could be linked to the endothelial dysfunction observed in NZO mice as a Pyk2 inhibitor was able to decrease eNOS Tyr656 phosphorylation to alleviate endothelial dysfunction and impaired NO production in vivo. This suggests that inhibition of Pyk2 results in the restoration of eNOS function in diabetes.

4.2 | Pyk2 inhibition restores the diabetes-induced impairment of endothelial function and cardioprotection

The importance of the endothelium for remote tissue protection mediated by increased NO bioavailability has been widely discussed (Bøtker et al., 2018; Davidson et al., 2019; Erkens et al., 2021; Hausenloy et al., 2019; Heusch, 2020). In line with this, our data showed an elevation of nitrite in the plasma from healthy humans after rIPC. rIPC is known to reduce the infarct size (Heusch, 2020; Heusch et al., 2015) but fails to exert protective effects in humans with diabetes and AMI (Hausenloy et al., 2019b). At the same time, we found no relevant elevations of plasma nitrite after applying rIPC to diabetic humans. Therapeutic strategies to reverse type 2 diabetes-induced alterations are lacking (Heusch, 2020). Diabetes and insulin resistance are associated with severe endothelial dysfunction due to eNOS impairment (Gupta et al., 2012; Kim et al., 2006). Our in vivo analyses of endothelial function by FMD showed a poor response to an increase in shear stress in diabetic NZO mice. Ex vivo assessment of endothelium-dependent relaxation of aortic rings confirmed these results. We and others have previously demonstrated that the pharmacological inhibition or gene knockdown of Pyk2 improves endothelial function and increases eNOS activity in vitro (Bibli et al., 2017; Viswambharan et al., 2017). The data presented in this study are the first to highlight the crucial role of Pyk2 in regulating endothelial function, eNOS activity, and systemic haemodynamics in vivo in a model of diabetes.

Multiple studies suggest that the endothelium releases factors with a protective effect on cardiomyocytes. Previously, we established that the endothelium partially contributes to rIPC-mediated remote cardioprotection by increasing circulating NO metabolite levels in plasma (Rassaf et al., 2014). Our transfer experiments indicated that there are plasma transports signals for cardioprotection, and that the tissue-protective effects of these signals in plasma are abolished in mice and humans with diabetes. The humans whose plasma was used for analysis in our study displayed the full range of diabetic features but exhibited a normoglycaemic state at the time of blood collection. However, the features of diabetes that impair these plasma-transmitted signals remain unclear, and their implications might differ. In previous studies, differences in LV function and oxidative stress were observed between obese nondiabetic patients and diabetic humans (Montaigne et al., 2014). In contrast, several parameters of myocardial respiration displayed a negative relationship to the severity of insulin resistance (Jelenik et al., 2018). Based on our data, tissue-protective signals in plasma are impaired in humans with diabetes, while these signals might be preserved in the early stages of insulin resistance. Several factors other than the endothelium are involved in signalling pathways responsible for rIPC-mediated cardioprotection. In addition to humoral and cellular factors, the neuronal pathway impacts remote tissue cardioprotection (Lieder et al., 2018) but may also be altered in diabetes (Pickard et al., 2016). In a similar approach to our interspecies transfer experiments, it was recently demonstrated that the cardioprotective signal released by rIPC was lacking in diabetic patients with polyneuropathy (Jensen et al., 2012). Our data support the notion that neuronal pathways play an important role in remote tissue cardioprotection, at least under healthy conditions. In contrast, we show evidence in diabetic NZO mice that neuronal signalling pathways have no impact on the infarct size, whereas inhibition of Pyk2 promotes rIPC-mediated cardioprotection.

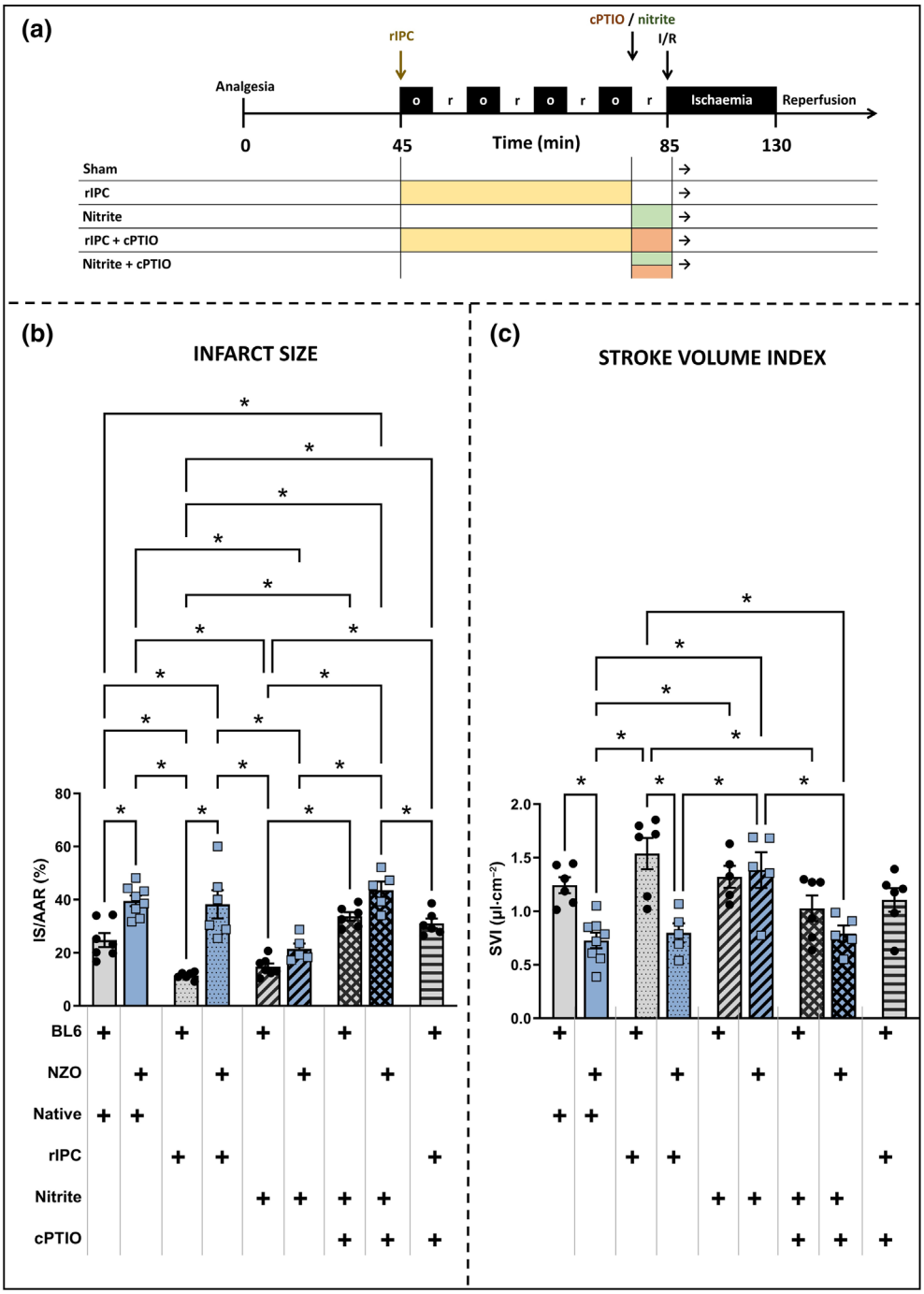

FIGURE 4 Larger infarct sizes and impaired endothelium-dependent remote cardioprotection (rIPC) in diabetes. (a) Schematic representation of the study protocols. (b) The infarct size (IS) per area at risk (AAR) of BL6 and diabetic NZO mice in accordance with different treatments highlighted under the bars. (c) Corresponding stroke volume indices (SVIs) of the respective intervention groups measured by echocardiography. rIPC reduced the infarct size in BL6 mice and improved left ventricular function, while this cardioprotective effect was not observed in diabetic NZO mice. Nitrite, as an exogenous reservoir of NO, had no effect in BL6 mice but reduced the infarct size in diabetic NZO mice. Coadministration of the NO scavenger cPTIO with nitrite selectively abolished the cardioprotective effects of rIPC and nitrite in BL6 mice and the beneficial effects of nitrite in diabetic NZO mice. "native" reffers to non-conditioned plasma. (b) Statistical significance was analysed by ordinary one-way ANOVA followed by Tukey's multiple comparisons test. $n_{BL6\ +\ native} = 7$, $n_{BL6\ +\ rIPC} = 6$, $n_{BL6\ +\ Nitrite} = 7$, $n_{BL6\ +\ Nitrite+cPTIO} = 6$, $n_{BL6\ +\ rIPC+cPTIO} = 6$, $n_{NZO\ +\ native} = 8$, $n_{NZO\ +\ rIPC} = 6$, $n_{NZO\ +\ Nitrite} = 5$, $n_{NZO\ +\ Nitrite+cPTIO} = 5$. $^*P < 0.05$. (c) Statistical significance was analysed by ordinary one-way ANOVA followed by Tukey's multiple comparisons test. $n_{BL6\ +\ native} = 6$, $n_{BL6\ +\ rIPC} = 6$, $n_{BL6\ +\ Nitrite} = 5$, $n_{BL6\ +\ Nitrite+cPTIO} = 6$, $n_{BL6\ +\ rIPC+cPTIO} = 6$, $n_{NZO\ +\ native} = 8$, $n_{NZO\ +\ rIPC} = 5$, $n_{NZO\ +\ Nitrite} = 5$, $n_{NZO\ +\ Nitrite+cPTIO} = 5$. $^*P < 0.05$.

TABLE 1 Left ventricular function measured by echocardiography in BL6 and diabetic NZO mice subjected to acute myocardial infarction (AMI).

BL6												
	Sham (n = 6)			rIPC (n = 6)			Nitrite (n = 5)			rIPC + cPTIO (n = 6)		
(A)	Baseline	Post-AMI	*P*-value	Baseline	Post-AMI	*P*-value	Baseline	Post-AMI	*P*-value	Baseline	Post-AMI	*P*-value
Heart rate (HR), bpm	407 ± 25	463 ± 51	0.1892	449 ± 30	493 ± 48	0.4261	467 ± 39	433 ± 65	0.7855	468 ± 47	463 ± 55	>0.9999
Ejection fraction (EF), %	56.1 ± 3.4	38.4 ± 4.8	**0.0096**	51.5 ± 19.5	40.7 ± 9.2	0.2261	51.2 ± 7.5	43.6 ± 3.8	0.6976	54.1 ± 3.6	35.2 ± 6.9	**0.0050**
End-systolic volume index (ESVI), µl·cm^{-2}	1.3 ± 0.1	2 ± 0.4	**0.0248**	1.6 ± 0.8	2.3 ± 0.7	0.0340	1.6 ± 0.3	1.8 ± 0.5	0.9844	1.5 ± 0.2	2 ± 0.3	0.0967
End-diastolic volume index (EDVI), µl·cm^{-2}	3 ± 0.1	3.3 ± 0.4	0.8789	3.2 ± 0.9	3.8 ± 0.8	0.0884	3.3 ± 0.6	3.1 ± 0.7	0.9650	3.2 ± 0.6	3.1 ± 0.4	0.9997
Stroke volume index (SVI), µl·cm^{-2}	1.7 ± 0.1	1.2 ± 0.2	**0.0434**	1.6 ± 0.5	1.5 ± 0.4	0.9983	1.7 ± 0.5	1.3 ± 0.2	0.2083	1.7 ± 0.4	1.1 ± 0.3	**0.0017**
Cardiac output index (COI), ml·min^{-1}·cm^{-2}	0.7 ± 0.1	0.6 ± 0.1	0.8998	0.7 ± 0.2	0.8 ± 0.2	0.9973	0.8 ± 0.2	0.6 ± 0.1	0.1216	0.8 ± 0.2	0.5 ± 0.1	**0.0030**

TABLE 1 (Continued)

BL6						
	Nitrite + cPTIO (n = 6)			Pyk2 inhibitor (n = 6)		
(A)	Baseline	Post-AMI	*P*-value	Baseline	Post-AMI	*P*-value
Heart rate (HR), bpm	453 ± 74	483 ± 32	0.8190	479 ± 35	479 ± 33	>0.9999
Ejection fraction (EF), %	58.6 ± 6.2	37.4 ± 3.3	**0.0015**	58.2 ± 7.8	44 ± 6.2	0.0514
End-systolic volume index (ESVI), µl·cm^{-2}	1.2 ± 0.3	1.7 ± 0.5	0.1210	1.2 ± 0.2	1.5 ± 0.4	0.5074
End-diastolic volume index (EDVI), µl·cm^{-2}	2.8 ± 0.4	2.8 ± 0.8	0.9994	2.9 ± 0.5	2.7 ± 0.6	0.9966
Stroke volume index (SVI), µl·cm^{-2}	1.7 ± 0.2	1 ± 0.3	**0.0021**	1.7 ± 0.4	1.2 ± 0.3	**0.0244**
Cardiac output index (COI), ml·min^{-1}·cm^{-2}	0.8 ± 0.2	0.5 ± 0.2	**0.0199**	0.8 ± 0.2	0.6 ± 0.2	**0.0395**

NZO												
	Sham (n = 8)			rIPC (n = 5)			Nitrite (n = 5)			Nitrite + cPTIO (n = 5)		
(B)	Baseline	Post-AMI	*P*-value	Baseline	Post-AMI	*P*-value	Baseline	Post-AMI	*P*-value	Baseline	Post-AMI	*P*-value
Heart rate (HR), bpm	443 ± 62	498 ± 67	0.0533	408 ± 46	429 ± 43	0.8709	453 ± 65	491 ± 59	0.4573	456 ± 27	440 ± 49	0.9509
Ejection fraction (EF), %	52.3 ± 8.2	27.7 ± 6.1	**<0.0001**	51 ± 7.8	30.7 ± 11.7	**0.0044**	41.8 ± 2.7	44.6 ± 16.5	0.9740	54.8 ± 11.4	37.4 ± 6.8	**0.0155**
End-systolic volume index (ESVI), µl·cm^{-2}	1.3 ± 0.3	1.9 ± 0.4	**0.0119**	1.3 ± 0.3	1.9 ± 0.6	**0.0444**	2.1 ± 0.4	1.9 ± 0.9	0.9454	1.1 ± 0.4	1.3 ± 0.2	0.7675
End-diastolic volume index (EDVI), µl·cm^{-2}	2.7 ± 0.4	2.6 ± 0.5	0.9489	2.6 ± 0.6	2.7 ± 0.6	0.9981	3.5 ± 0.6	3.3 ± 0.9	0.8280	2.4 ± 0.4	2.1 ± 0.3	0.7020
Stroke volume index (SVI), µl·cm^{-2}	1.4 ± 0.3	0.7 ± 0.2	**0.0002**	1.4 ± 0.4	0.8 ± 0.2	**0.0198**	1.5 ± 0.2	1.4 ± 0.4	0.9892	1.3 ± 0.3	0.8 ± 0.2	**0.0396**
Cardiac output index (COI), ml·min^{-1}·cm^{-2}	0.6 ± 0.2	0.4 ± 0.1	**0.0037**	0.5 ± 0.1	0.3 ± 0.1	0.1607	0.7 ± 0.1	0.7 ± 0.2	0.9980	0.6 ± 0.1	0.4 ± 0.1	**0.0628**

Note: The table shows left ventricular functional parameters of native BL6 (A) and diabetic NZO (B) mice before and after AMI and after administration of the different treatments. All treatment protocols are shown in Figure S2. All parameters besides heart rate and ejection fraction were normalized to the body surface area. Data shown as mean ± standard deviation. Statistical significance was assessed by repeated measurements two-way ANOVA with Šídák's multiple comparisons test for the timepoints. n-values are shown in the table headers. rIPC, remote ischaemic preconditioning. Bold emphasis highlights which comparisons are statistically significant.

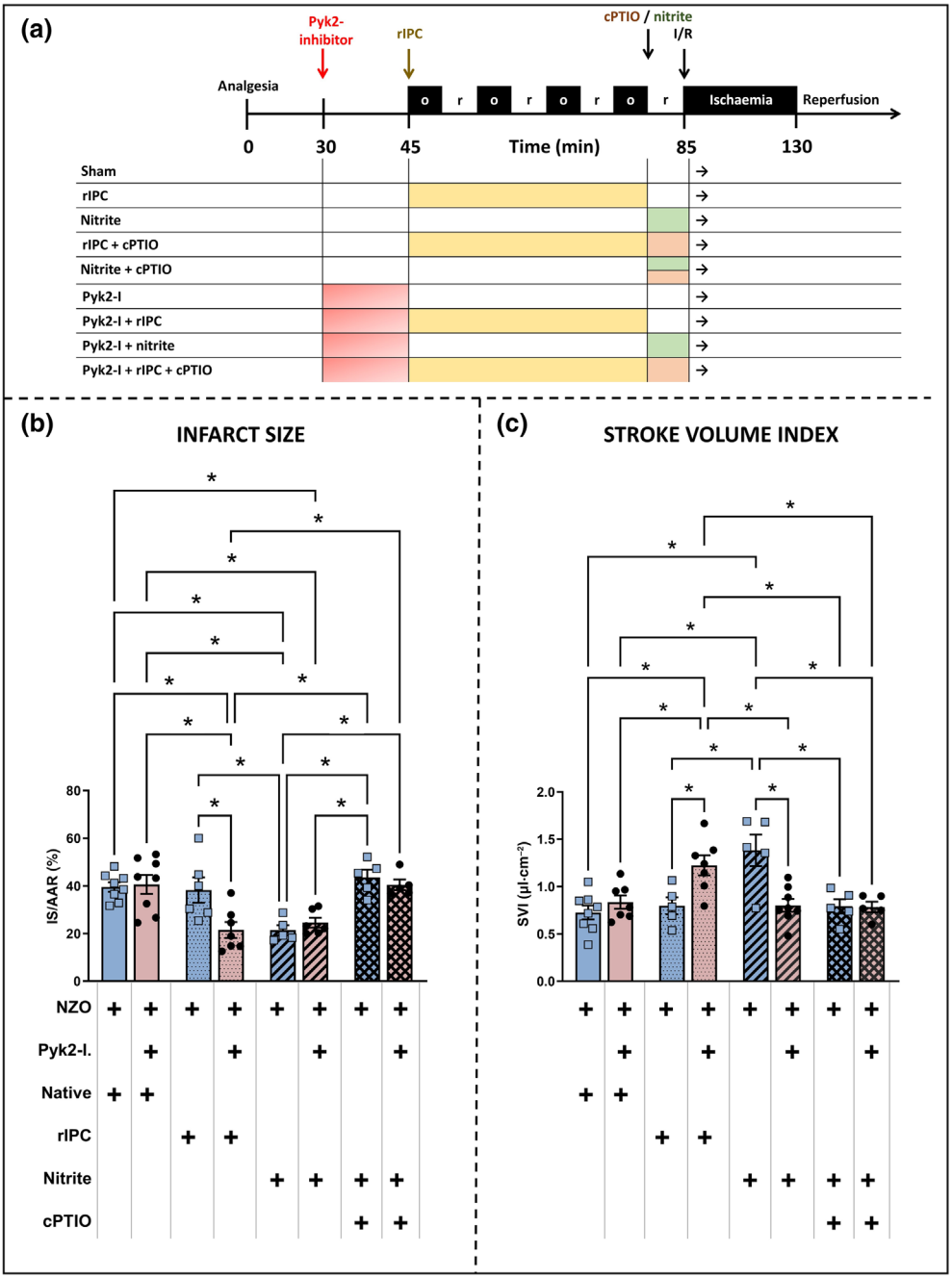

FIGURE 5 Pyk2 inhibition (Pyk2-I) restores endothelium-dependent remote cardioprotection (rIPC) in diabetes. (a) Schematic representation of the study protocols to which mice were subjected. The Pyk2 inhibitor was injected i.p. 15 min before the different protocols. (b) The infarct size (IS) per area at risk (AAR) in diabetic NZO mice treated with and without the Pyk2 inhibitor. (c) Corresponding stroke volume indices (SVIs) of the respective intervention groups. In diabetic NZO mice, Pyk2 inhibition restored the cardioprotective effects of rIPC, as indicated by smaller infarct sizes and improved SVIs. Administration of the NO scavenger cPTIO neutralized this cardioprotective effect, indicating that eNOS contributed to rIPC-dependent cardioprotection. Exogenous nitrite was cardioprotective but did not enhance the effect of rIPC. The groups of diabetic NZO mice shown in (b) and (c) coincide with the groups shown in Figure 4. "native" reffers to non-conditioned plasma (b) Statistical significance was analysed by ordinary one-way ANOVA followed by Tukey's multiple comparisons test. $n_{NZO + native} = 8$, $n_{NZO + rIPC} = 6$, $n_{NZO + Nitrite} = 5$, $n_{NZO + Nitrite+cPTIO} = 5$, $n_{NZO + Pyk2\text{-}I.} = 8$, $n_{NZO + Pyk2\text{-}I. + rIPC} = 7$, $n_{NZO + PYk2\text{-}I. + Nitrite} = 6$, $n_{NZO + Pyk2\text{-}I. + rIPC+cPTIO} = 5$. *$P < 0.05$. (c) Statistical significance was analysed by ordinary one-way ANOVA followed by Tukey's multiple comparisons test. $n_{NZO + native} = 8$, $n_{NZO + rIPC} = 5$, $n_{NZO + Nitrite} = 5$, $n_{NZO + Nitrite+cPTIO} = 5$, $n_{NZO + Pyk2\text{-}I.} = 7$, $n_{NZO + Pyk2\text{-}I. + rIPC} = 7$, $n_{NZO + PYk2\text{-}I. + Nitrite} = 8$, $n_{NZO + Pyk2\text{-}I. + rIPC+cPTIO} = 5$. *$P < 0.05$.

The in vivo results demonstrated an increase in the infarct size, whereas the rIPC-dependent decrease in the infarct size was abrogated in diabetic NZO mice compared to BL6 mice after myocardial ischaemia/reperfusion. Notably, the effect size of Pyk2 inhibition in restoring the cardioprotective effect of rIPC was considerable, with Pyk2 inhibition resulting in almost complete elimination of the

TABLE 2 Left ventricular function measured by echocardiography in diabetic NZO mice receiving systemic injection of a Pyk2 inhibitor and subjected to acute myocardial infarction (AMI).

NZO + Pyk2 inhibitor	Sham (n = 7)			rIPC (n = 7)			Nitrite (n = 8)			rIPC + cPTIO (n = 5)		
	Baseline	Post-AMI	*P*-value	Baseline	Post-AMI	*P*-value	Baseline	Post-AMI	*P*-value	Baseline	Post-AMI	*P*-value
Heart rate (HR), bpm	462 ± 38	434 ± 68	0.8577	437 ± 71	473 ± 59	0.7050	411 ± 72	486 ± 33	0.0778	465 ± 51	449 ± 51	0.9887
Ejection fraction (EF), %	48.3 ± 8.9	29.9 ± 4.5	**<0.0001**	47.7 ± 4	45.4 ± 5.7	0.8490	57.2 ± 8.1	52.4 ± 9	0.2177	52.5 ± 2.7	33.2 ± 5.8	**<0.0001**
End-systolic volume index (ESVI), $\mu l \cdot cm^{-2}$	1.4 ± 0.3	2.0 ± 0.3	**0.0012**	1.5 ± 0.2	1.5 ± 0.3	0.9948	0.8 ± 0.2	0.7 ± 0.2	0.9960	1.1 ± 0.2	1.6 ± 0.4	**0.0166**
End-diastolic volume index (EDVI), $\mu l \cdot cm^{-2}$	2.7 ± 0.4	2.8 ± 0.4	0.9878	2.9 ± 0.5	2.7 ± 0.5	0.7980	1.8 ± 0.4	1.5 ± 0.3	0.6288	2.4 ± 0.4	2.4 ± 0.4	0.9997
Stroke volume index (SVI), $\mu l \cdot cm^{-2}$	1.3 ± 0.3	0.8 ± 0.2	**0.0058**	1.4 ± 0.3	1.2 ± 0.3	0.5747	1 ± 0.3	0.8 ± 0.2	0.2891	1.2 ± 0.3	0.8 ± 0.1	**0.0273**
Cardiac output index (COI), $ml \cdot min^{-1} \cdot cm^{-2}$	0.6 ± 0.1	0.4 ± 0.1	**0.0067**	0.6 ± 0.1	0.6 ± 0.2	0.9925	0.4 ± 0.1	0.4 ± 0.1	0.9880	0.6 ± 0.2	0.4 ± 0.1	**0.0228**

Note: The table shows the left ventricular functional parameters of diabetic NZO mice receiving systemic injection of a Pyk2 inhibitor before and after acute myocardial infarction (AMI) and after the different treatments. A Pyk2 inhibitor was administered intraperitoneally 15 min before treatment. All treatment protocols are shown in Figure S2. All parameters besides heart rate and ejection fraction were normalized to the body surface area. Data shown as mean ± standard deviation. Statistical significance was assessed by repeated measurements two-way ANOVA with Šídák's multiple comparisons test for the timepoints. n-values are shown in the table headers. rIPC, remote ischaemic preconditioning. Bold emphasis highlights which comparisons are statistically significant.

diabetes-associated enlargement of infarct size. The regulation of eNOS activation is shear stress- and time-course-dependent (Bibli et al., 2017; Inserte et al., 2013). The reduction in infarct size in Pyk2 inhibitor-treated diabetic NZO mice after rIPC may have also been modulated by the coronary endothelium (Bice et al., 2016). The infarct size was not reduced in BL6 or diabetic NZO mice receiving the Pyk2 inhibitor alone. These results support the notion that the vascular endothelium in the hindlimbs exerts protective effects. The results of the experiments involving transfer of plasma from mice and humans subjected to rIPC demonstrate that inhibition of eNOS by Pyk2 in remote endothelium plays a fundamental role in the loss of endothelium-dependent rIPC-mediated cardioprotection in diabetes. Translating preconditioning to clinical practice might prove challenging due to the unpredictability of coronary occlusions (Heusch, 2023). However, preconditioning offers a more viable option for clinical application, a topic that future trials will need to explore (Heusch, 2024). Taken together, these data show that Pyk2 inhibition contributes to limiting the infarct size by restoring endothelium-dependent rIPC-induced cardioprotection in diabetes.

5 | LIMITATIONS

The current study has some limitations that must be addressed. First, restoration of endothelium-dependent cardioprotection by rIPC was examined by the pharmacological inhibition of Pyk2 and not by gene knock-out. PF-431396 hydrate inhibits, besides Pyk2, several kinases, including **FAK**, which might be interconnected in ischaemic preconditioning. However, it seems that FAK activation rather than FAK inhibition would elicit beneficial effect of preconditioning (Cheng et al., 2012; Perricone et al., 2013). In addition, the feasibility and safety of developing pharmacological Pyk2 inhibitors for human use may be challenging in controlling specificity and managing possible side effects due to inhibition of other kinases. Second, we compared the diabetic NZO mice with BL6 mice to contrast a diabetes-prone from a diabetes-resistant strain. NZO mice are an inbred strain representing a polygenic model for diabetes without specific single-risk gene modifications, meaning a traditional genetic control group does not apply. While diabetic NZO mice exhibit key diabetes characteristics, they may not fully reflect the human disease's cellular and systemic complexity. Despite potential genomic variation confounders, our cardiac function assessments yielded consistent results across strains, providing a reliable baseline for comparison. Third, our vasoreactivity studies were performed on thoracic aortic segments, whereas rIPC and FMD were performed on smaller vessels in the hindlimb. Fourth, we analysed the effects in male mice, therefore our results cannot be transposed on female mice, although, recently, no gender-specific differences regarding infarct size and its reduction by rIPC was observed in minipigs (Kleinbongard et al., 2022). Moreover, the hybrid transfer experiments involved individuals with diabetes, along with comorbidities like hypercholesterolemia, obesity, and coronary artery disease. These accompanying conditions could potentially contribute to the reduced effectiveness of rIPC. Notably, despite age

potentially affecting rIPC effectiveness, we observed an effect of plasma from age-matched, non-diabetic humans treated with rIPC. In addition, we did not search for simultaneous changes in the inducible nitric oxide synthase (iNOS) and the neuronal nitric oxide synthase (nNOS) in local endothelial cells exposed to rIPC or in the remote myocardium. Lastly, we performed Western Blotting in lung tissue for increasing the amount of endothelial cells by tissue preparation. Interpretation and transposition of this data on other tissues should be carried out with caution.

6 | CONCLUSION

Endothelial cell function and its contribution to remote tissue protection are severely impaired in diabetes. Pyk2 is activated in diabetic mice. Targeting Pyk2 rescued eNOS function, NO generation and the cardioprotective effects of rIPC in diabetic conditions. The inhibition of Pyk2 may be a novel strategy to treat endothelial dysfunction and to restore endothelial dependent remote tissue protection in diabetes.

AUTHOR CONTRIBUTIONS

R. Erkens, H. Al-Hasani and M. Kelm designed the study. A. Chadt and H. Al-Hasani provided mice for the study. R. Erkens, D. A. Duse, A. Brum, S. Becher, M. Siragusa, C. Quast and J. Müssig performed experiments, collected data and analysed it; R. Erkens, D. A. Duse and A. Brum interpreted data with the input of M. Kelm, M. Cortese-Krott, I. Fleming, H. Al-Hasani, M. Roden, C. Jung and G. Heusch; R. Erkens, D. A. Duse and M. Kelm prepared the original draft. C. Jung, M. Cortese-Krott, B. Ibáñez and E. Lammert reviewed and edited the manuscript. All authors have read and agreed to the published version of the manuscript.

AFFILIATIONS

[1]Department of Cardiology, Pulmonology and Vascular Medicine, Medical Faculty, Heinrich Heine University, Duesseldorf, Germany
[2]Institute for Clinical Biochemistry and Pathobiochemistry, Deutsches Diabetes Zentrum at Heinrich Heine University of Duesseldorf, Duesseldorf, Germany
[3]German Center for Diabetes Research (DZD e.V.), Partner Duesseldorf, Neuherberg, Germany
[4]Center for Molecular Medicine, Institute for Vascular Signalling, Goethe University Frankfurt, Frankfurt, Germany
[5]German Centre for Cardiovascular Research, Partner site RhineMain, Frankfurt, Germany
[6]Department of Endocrinology and Diabetology, Medical Faculty, Heinrich-Heine University and University Hospital Duesseldorf, Duesseldorf, Germany
[7]Institute for Clinical Diabetology, Deutsches Diabetes Zentrum at Heinrich Heine University of Duesseldorf, Duesseldorf, Germany
[8]CARID Cardiovascular Research Institute Duesseldorf, Duesseldorf, Germany
[9]Centro de Investigación Biomédica en Red de Enfermedades Cardiovasculares (CIBERCV), Madrid, Spain
[10]Institute of Metabolic Physiology, Heinrich-Heine University, Duesseldorf, Germany
[11]Institute for Pathophysiology, West German Heart and Vascular Center, University School of Medicine Essen, Essen, Germany

ACKNOWLEDGEMENTS

The authors wish to thank Dr. Jennifer Dirzka for technical assistance in the preparation of the organ bath experiments and to Dr. Ramesh Chennupati and Mrs. Katerina Askeridis for their technical support in some experiments. Open Access funding enabled and organized by Projekt DEAL.

CONFLICT OF INTEREST STATEMENT

None.

DATA AVAILABILITY STATEMENT

The data that support the findings of this study are available from the corresponding author upon reasonable request.

DECLARATION OF TRANSPARENCY AND SCIENTIFIC RIGOUR

This Declaration acknowledges that this paper adheres to the principles for transparent reporting and scientific rigour of preclinical research as stated in the *BJP* guidelines for Natural Products Research, Design and Analysis, Immunoblotting and Immunochemistry, and Animal Experimentation, and as recommended by funding agencies, publishers and other organizations engaged with supporting research.

ORCID

Ralf Erkens https://orcid.org/0000-0002-3373-652X
Miriam Cortese-Krott https://orcid.org/0000-0002-0593-1192
Borja Ibáñez https://orcid.org/0000-0002-5036-254X

REFERENCES

Ahlqvist, E., Storm, P., Käräjämäki, A., Martinell, M., Dorkhan, M., Carlsson, A., Vikman, P., Prasad, R. B., Aly, D. M., Almgren, P., Wessman, Y., Shaat, N., Spégel, P., Mulder, H., Lindholm, E., Melander, O., Hansson, O., Malmqvist, U., Lernmark, Å., … Groop, L. (2018). Novel subgroups of adult-onset diabetes and their association with outcomes: A data-driven cluster analysis of six variables. *The Lancet Diabetes & Endocrinology*, *6*, 361–369. https://doi.org/10.1016/S2213-8587(18)30051-2

Alexander, S. P. H., Christopoulos, A., Davenport, A. P., Kelly, E., Mathie, A. A., Peters, J. A., Veale, E. L., Armstrong, J. F., Faccenda, E., Harding, S. D., Davies, J. A., Abbracchio, M. P., Abraham, G., Agoulnik, A., Alexander, W., Al-Hosaini, K., Bäck, M., Baker, J. G., Barnes, N. M., … Ye, R. D. (2023). The Concise Guide to PHARMACOLOGY 2023/24: G protein-coupled receptors. *British Journal of Pharmacology*, *180*, S23–S144. https://doi.org/10.1111/bph.16177

Alexander, S. P. H., Fabbro, D., Kelly, E., Mathie, A. A., Peters, J. A., Veale, E. L., Armstrong, J. F., Faccenda, E., Harding, S. D., Davies, J. A., Annett, S., Boison, D., Burns, K. E., Dessauer, C., Gertsch, J., Helsby, N. A., Izzo, A. A., Ostrom, R., Papapetropoulos, A., … Wong, S. S. (2023). The concise guide to pharmacology 2023/24: Enzymes. *British Journal of Pharmacology*, *180*(Suppl 2), S289–s373.

Alexander, S. P. H., Roberts, R. E., Broughton, B. R. S., Sobey, C. G., George, C. H., Stanford, S. C., Cirino, G., Docherty, J. R.,

Giembycz, M. A., Hoyer, D., Insel, P. A., Izzo, A. A., Ji, Y., MacEwan, D. J., Mangum, J., Wonnacott, S., & Ahluwalia, A. (2018). Goals and practicalities of immunoblotting and immunohistochemistry: A guide for submission to the *British Journal of Pharmacology*. *British Journal of Pharmacology*, *175*, 407–411. https://doi.org/10.1111/bph.14112

Bibli, S. I., Zhou, Z., Zukunft, S., Fisslthaler, B., Andreadou, I., Szabo, C., Brouckaert, P., Fleming, I., & Papapetropoulos, A. (2017). Tyrosine phosphorylation of eNOS regulates myocardial survival after an ischaemic insult: Role of PYK2. *Cardiovascular Research*, *113*, 926–937. https://doi.org/10.1093/cvr/cvx058

Bice, J. S., Jones, B. R., Chamberlain, G. R., & Baxter, G. F. (2016). Nitric oxide treatments as adjuncts to reperfusion in acute myocardial infarction: A systematic review of experimental and clinical studies. *Basic Research in Cardiology*, *111*, 23. https://doi.org/10.1007/s00395-016-0540-y

Bielschowsky, F., & Bielschowsky, M. (1956). The New Zealand strain of obese mice; their response to stilboestrol and to insulin. *The Australian Journal of Experimental Biology and Medical Science*, *34*, 181–198. https://doi.org/10.1038/icb.1956.22

Bøtker, H. E., Hausenloy, D., Andreadou, I., Antonucci, S., Boengler, K., Davidson, S. M., Deshwal, S., Devaux, Y., di Lisa, F., di Sante, M., Efentakis, P., Femminò, S., García-Dorado, D., Giricz, Z., Ibanez, B., Iliodromitis, E., Kaludercic, N., Kleinbongard, P., Neuhäuser, M., … Heusch, G. (2018). Practical guidelines for rigor and reproducibility in preclinical and clinical studies on cardioprotection. *Basic Research in Cardiology*, *113*, 39. https://doi.org/10.1007/s00395-018-0696-8

Cheng, Z., DiMichele, L. A., Hakim, Z. S., Rojas, M., Mack, C. P., & Taylor, J. M. (2012). Targeted focal adhesion kinase activation in cardiomyocytes protects the heart from ischaemia/reperfusion injury. *Arteriosclerosis, Thrombosis, and Vascular Biology*, *32*, 924–933. https://doi.org/10.1161/ATVBAHA.112.245134

Curtis, M. J., Alexander, S. P. H., Cirino, G., George, C. H., Kendall, D. A., Insel, P. A., Izzo, A. A., Ji, Y., Panettieri, R. A., Patel, H. H., Sobey, C. G., Stanford, S. C., Stanley, P., Stefanska, B., Stephens, G. J., Teixeira, M. M., Vergnolle, N., & Ahluwalia, A. (2022). Planning experiments: Updated guidance on experimental design and analysis and their reporting III. *British Journal of Pharmacology*, *179*(15), 3907–3913. https://doi.org/10.1111/bph.15868

Davidson, S. M., Ferdinandy, P., Andreadou, I., Bøtker, H. E., Heusch, G., Ibáñez, B., Ovize, M., Schulz, R., Yellon, D. M., Hausenloy, D. J., Garcia-Dorado, D., & CARDIOPROTECTION COST Action (CA16225). (2019). Multitarget strategies to reduce myocardial ischemia/reperfusion injury: JACC review topic of the week. *Journal of the American College of Cardiology*, *73*, 89–99. https://doi.org/10.1016/j.jacc.2018.09.086

Donato, A. J., Eskurza, I., Silver, A. E., Levy, A. S., Pierce, G. L., Gates, P. E., & Seals, D. R. (2007). Direct evidence of endothelial oxidative stress with aging in humans: Relation to impaired endothelium-dependent dilation and upregulation of nuclear factor-kappaB. *Circulation Research*, *100*, 1659–1666. https://doi.org/10.1161/01.RES.0000269183.13937.e8

Dreja, T., Jovanovic, Z., Rasche, A., Kluge, R., Herwig, R., Tung, Y. C., Joost, H. G., Yeo, G. S. H., & al-Hasani, H. (2010). Diet-induced gene expression of isolated pancreatic islets from a polygenic mouse model of the metabolic syndrome. *Diabetologia*, *53*, 309–320. https://doi.org/10.1007/s00125-009-1576-4

Emerging Risk Factors Collaboration, Sarwar, N., Gao, P., Seshasai, S. R., Gobin, R., Kaptoge, S., di Angelantonio, E., Ingelsson, E., Lawlor, D. A., Selvin, E., Stampfer, M., Stehouwer, C. D., Lewington, S., Pennells, L., Thompson, A., Sattar, N., White, I. R., Ray, K. K., & Danesh, J. (2010). Diabetes mellitus, fasting blood glucose concentration, and risk of vascular disease: A collaborative meta-analysis of 102 prospective studies. *Lancet*, *375*, 2215–2222. https://doi.org/10.1016/S0140-6736(10)60484-9

Erkens, R., Kramer, C. M., Lückstädt, W., Panknin, C., Krause, L., Weidenbach, M., Dirzka, J., Krenz, T., Mergia, E., Suvorava, T., Kelm, M., & Cortese-Krott, M. M. (2015). Left ventricular diastolic dysfunction in Nrf2 knock out mice is associated with cardiac hypertrophy, decreased expression of SERCA2a, and preserved endothelial function. *Free Radical Biology & Medicine*, *89*, 906–917. https://doi.org/10.1016/j.freeradbiomed.2015.10.409

Erkens, R., Suvorava, T., Sutton, T. R., Fernandez, B. O., Mikus-Lelinska, M., Barbarino, F., Flögel, U., Kelm, M., Feelisch, M., & Cortese-Krott, M. M. (2018). Nrf2 deficiency unmasks the significance of nitric oxide synthase activity for cardioprotection. *Oxidative Medicine and Cellular Longevity*, *2018*, 8309698.

Erkens, R., Totzeck, M., Brum, A., Duse, D., Bøtker, H. E., Rassaf, T., & Kelm, M. (2021). Endothelium-dependent remote signaling in ischemia and reperfusion: Alterations in the cardiometabolic continuum. *Free Radical Biology & Medicine*, *165*, 265–281. https://doi.org/10.1016/j.freeradbiomed.2021.01.040

Feige, K., Roth, S., M'Pembele, R., Galow, A., Koenig, S., Stroethoff, M., Raupach, A., Lurati Buse, G., Mathes, A. M., Hollmann, M. W., Huhn, R., & Torregroza, C. (2022). Influence of short and long hyperglycemia on cardioprotection by remote ischemic preconditioning—A translational approach. *International Journal of Molecular Sciences*, *23*, 14557. https://doi.org/10.3390/ijms232314557

Ferdinandy, P., Andreadou, I., Baxter, G. F., Bøtker, H. E., Davidson, S. M., Dobrev, D., Gersh, B. J., Heusch, G., Lecour, S., Ruiz-Meana, M., Zuurbier, C. J., Hausenloy, D. J., & Schulz, R. (2023). Interaction of cardiovascular nonmodifiable risk factors, comorbidities and comedications with ischemia/reperfusion injury and cardioprotection by pharmacological treatments and ischemic conditioning. *Pharmacological Reviews*, *75*, 159–216. https://doi.org/10.1124/pharmrev.121.000348

Fisslthaler, B., Loot, A. E., Mohamed, A., Busse, R., & Fleming, I. (2008). Inhibition of endothelial nitric oxide synthase activity by proline-rich tyrosine kinase 2 in response to fluid shear stress and insulin. *Circulation Research*, *102*, 1520–1528. https://doi.org/10.1161/CIRCRESAHA.108.172072

Fleming, I., Fisslthaler, B., Dimmeler, S., Kemp, B. E., & Busse, R. (2001). Phosphorylation of Thr(495) regulates Ca(2+)/calmodulin-dependent endothelial nitric oxide synthase activity. *Circulation Research*, *88*, E68–E75.

Fleming, I., Schulz, C., Fichtlscherer, B., Kemp, B. E., Fisslthaler, B., & Busse, R. (2003). AMP-activated protein kinase (AMPK) regulates the insulin-induced activation of the nitric oxide synthase in human platelets. *Thrombosis and Haemostasis*, *90*, 863–871.

Flögel, U., Decking, U. K., Gödecke, A., & Schrader, J. (1999). Contribution of NO to ischemia-reperfusion injury in the saline-perfused heart: A study in endothelial NO synthase knockout mice. *Journal of Molecular and Cellular Cardiology*, *31*, 827–836. https://doi.org/10.1006/jmcc.1998.0921

Frank, G. D., & Eguchi, S. (2003). Activation of tyrosine kinases by reactive oxygen species in vascular smooth muscle cells: Significance and involvement of EGF receptor transactivation by angiotensin II. *Antioxidants & Redox Signaling*, *5*, 771–780. https://doi.org/10.1089/152308603770380070

Fulton, D., Ruan, L., Sood, S. G., Li, C., Zhang, Q., & Venema, R. C. (2008). Agonist-stimulated endothelial nitric oxide synthase activation and vascular relaxation. Role of eNOS phosphorylation at Tyr83. *Circulation Research*, *102*, 497–504. https://doi.org/10.1161/CIRCRESAHA.107.162933

Gödecke, A., Decking, U. K. M., Ding, Z., Hirchenhain, J., Bidmon, H.-J., Gödecke, S., & Schrader, J. (1998). Coronary hemodynamics in endothelial NO synthase knockout mice. *Circulation Research*, *82*, 186–194. https://doi.org/10.1161/01.RES.82.2.186

Gupta, A. K., Ravussin, E., Johannsen, D. L., Stull, A. J., Cefalu, W. T., & Johnson, W. D. (2012). Endothelial dysfunction: An early

cardiovascular risk marker in asymptomatic obese individuals with pre-diabetes. *British Journal of Medicine and Medical Research*, *2*, 413–423. https://doi.org/10.9734/BJMMR/2012/1479

Haskell, B. D., Flurkey, K., Duffy, T. M., Sargent, E. E., & Leiter, E. H. (2002). The diabetes-prone NZO/HlLt strain. I. Immunophenotypic comparison to the related NZB/BINJ and NZW/LacJ strains. *Laboratory Investigation; a Journal of Technical Methods and Pathology*, *82*, 833–842. https://doi.org/10.1097/01.LAB.0000018915.53257.00

Hausenloy, D. J., Kharbanda, R. K., Møller, U. K., Ramlall, M., Aarøe, J., Butler, R., Bulluck, H., Clayton, T., Dana, A., Dodd, M., Engstrom, T., Evans, R., Lassen, J. F., Christensen, E. F., Garcia-Ruiz, J. M., Gorog, D. A., Hjort, J., Houghton, R. F., Ibanez, B., … Collier, L. (2019). Effect of remote ischaemic conditioning on clinical outcomes in patients with acute myocardial infarction (CONDI-2/ERIC-PPCI): A single-blind randomised controlled trial. *Lancet (London, England)*, *394*, 1415–1424. https://doi.org/10.1016/S0140-6736(19)32039-2

Heusch, G. (2020). Myocardial ischaemia-reperfusion injury and cardioprotection in perspective. *Nature Reviews Cardiology*, *17*, 773–789. https://doi.org/10.1038/s41569-020-0403-y

Heusch, G. (2023). Cardioprotection and its translation: A need for new paradigms? Or for new pragmatism? An opinionated retro- and perspective. *Journal of Cardiovascular Pharmacology and Therapeutics*, *28*, 10742484231179613.

Heusch, G. (2024). Myocardial ischemia/reperfusion: Translational pathophysiology of ischemic heart disease. *Med*, *5*, 10–31.

Heusch, G., Bøtker, H. E., Przyklenk, K., Redington, A., & Yellon, D. (2015). Remote ischemic conditioning. *Journal of the American College of Cardiology*, *65*, 177–195. https://doi.org/10.1016/j.jacc.2014.10.031

Inserte, J., Hernando, V., Vilardosa, Ú., Abad, E., Poncelas-Nozal, M., & Garcia-Dorado, D. (2013). Activation of cGMP/protein kinase G pathway in postconditioned myocardium depends on reduced oxidative stress and preserved endothelial nitric oxide synthase coupling. *Journal of the American Heart Association*, *2*, e005975. https://doi.org/10.1161/JAHA.112.005975

Izzo, A. A., Teixeira, M., Alexander, S. P., Cirino, G., Docherty, J. R., George, C. H., Insel, P. A., Ji, Y., Kendall, D. A., Panattieri, R. A., Sobey, C. G., Stanford, S. C., Stefanska, B., Stephens, G., & Ahluwalia, A. (2020). A practical guide for transparent reporting of research on natural products in the *British Journal of Pharmacology*: Reproducibility of natural product research. *British Journal of Pharmacology*, *177*(10), 2169–2178. https://doi.org/10.1111/bph.15054

Jelenik, T., Flögel, U., Álvarez-Hernández, E., Scheiber, D., Zweck, E., Ding, Z., Rothe, M., Mastrototaro, L., Kohlhaas, V., Kotzka, J., Knebel, B., Müller-Wieland, D., Moellendorf, S., Gödecke, A., Kelm, M., Westenfeld, R., Roden, M., & Szendroedi, J. (2018). Insulin resistance and vulnerability to cardiac ischemia. *Diabetes*, *67*, 2695–2702. https://doi.org/10.2337/db18-0449

Jensen, R. V., Støttrup, N. B., Kristiansen, S. B., & Bøtker, H. E. (2012). Release of a humoral circulating cardioprotective factor by remote ischemic preconditioning is dependent on preserved neural pathways in diabetic patients. *Basic Research in Cardiology*, *107*, 285. https://doi.org/10.1007/s00395-012-0285-1

Jonas, W., Kluth, O., Helms, A., Voß, S., Jähnert, M., Gottmann, P., Knebel, B., Chadt, A., al-Hasani, H., Schürmann, A., & Vogel, H. (2022). Identification of novel genes involved in hyperglycemia in mice. *International Journal of Molecular Sciences*, *23*, 3205. https://doi.org/10.3390/ijms23063205

Joost, H. G., & Schurmann, A. (2014). The genetic basis of obesity-associated type 2 diabetes (diabesity) in polygenic mouse models. *Mammalian Genome : Official Journal of the International Mammalian Genome Society*, *25*, 401–412. https://doi.org/10.1007/s00335-014-9514-2

Kalyani, R. R. (2021). Glucose-lowering drugs to reduce cardiovascular risk in type 2 diabetes. *The New England Journal of Medicine*, *384*, 1248–1260. https://doi.org/10.1056/NEJMcp2000280

Kim, J. A., Montagnani, M., Koh, K. K., & Quon, M. J. (2006). Reciprocal relationships between insulin resistance and endothelial dysfunction: Molecular and pathophysiological mechanisms. *Circulation*, *113*, 1888–1904. https://doi.org/10.1161/CIRCULATIONAHA.105.563213

Kleinbongard, P., Lieder, H., Skyschally, A., & Heusch, G. (2022). No sex-related differences in infarct size, no-reflow, and protection by ischaemic pre-conditioning in Göttingen minipigs. *Cardiovascular Research*, *119*, 561–570.

Kleinbongard, P., Skyschally, A., & Heusch, G. (2017). Cardioprotection by remote ischemic conditioning and its signal transduction. *Pflügers Archiv / European Journal of Physiology*, *469*, 159–181. https://doi.org/10.1007/s00424-016-1922-6

Kluge, R., Scherneck, S., Schürmann, A., & Joost, H. G. (2012). Pathophysiology and genetics of obesity and diabetes in the New Zealand obese mouse: A model of the human metabolic syndrome. *Methods in Molecular Biology*, *933*, 59–73. https://doi.org/10.1007/978-1-62703-068-7_5

Knebel, B., Göddeke, S., Hartwig, S., Hörbelt, T., Fahlbusch, P., al-Hasani, H., Jacob, S., Koellmer, C., Nitzgen, U., Schiller, M., Lehr, S., & Kotzka, J. (2018). Alteration of liver peroxisomal and mitochondrial functionality in the NZO mouse model of metabolic syndrome. *Proteomics Clinical Applications*, *12*, 1700028. https://doi.org/10.1002/prca.201700028

Kolb, H., Kempf, K., Röhling, M., & Martin, S. (2020). Insulin: Too much of a good thing is bad. *BMC Medicine*, *18*, 224. https://doi.org/10.1186/s12916-020-01688-6

Lieder, H. R., Kleinbongard, P., Skyschally, A., Hagelschuer, H., Chilian, W. M., & Heusch, G. (2018). Vago-splenic axis in signal transduction of remote ischemic preconditioning in pigs and rats. *Circulation Research*, *123*, 1152–1163. https://doi.org/10.1161/CIRCRESAHA.118.313859

Lilley, E., Stanford, S. C., Kendall, D. E., Alexander, S. P., Cirino, G., Docherty, J. R., George, C. H., Insel, P. A., Izzo, A. A., Ji, Y., Panettieri, R. A., Sobey, C. G., Stefanska, B., Stephens, G., Teixeira, M., & Ahluwalia, A. (2020). ARRIVE 2.0 and the *British Journal of Pharmacology*: Updated guidance for 2020. *British Journal of Pharmacology*, *177*, 3611–3616. https://bpspubs.onlinelibrary.wiley.com/doi/full/10.1111/bph.15178

Milazzo, V., Cosentino, N., Genovese, S., Campodonico, J., Mazza, M., de Metrio, M., & Marenzi, G. (2021). Diabetes mellitus and acute myocardial infarction: Impact on short and long-term mortality. *Advances in Experimental Medicine and Biology*, *1307*, 153–169. https://doi.org/10.1007/5584_2020_481

Mocanu, M. M., & Yellon, D. M. (2007). PTEN, the Achilles' heel of myocardial ischaemia/reperfusion injury? *British Journal of Pharmacology*, *150*, 833–838. https://doi.org/10.1038/sj.bjp.0707155

Montaigne, D., Marechal, X., Coisne, A., Debry, N., Modine, T., Fayad, G., Potelle, C., el Arid, J. M., Mouton, S., Sebti, Y., Duez, H., Preau, S., Remy-Jouet, I., Zerimech, F., Koussa, M., Richard, V., Neviere, R., Edme, J. L., Lefebvre, P., & Staels, B. (2014). Myocardial contractile dysfunction is associated with impaired mitochondrial function and dynamics in type 2 diabetic but not in obese patients. *Circulation*, *130*, 554–564. https://doi.org/10.1161/CIRCULATIONAHA.113.008476

Murphy, J. M., Jeong, K., Rodriguez, Y. A. R., Kim, J. H., Ahn, E. E., & Lim, S. S. (2019). FAK and Pyk2 activity promote TNF-α and IL-1β-mediated pro-inflammatory gene expression and vascular inflammation. *Scientific Reports*, *9*, 7617. https://doi.org/10.1038/s41598-019-44098-2

Ortlepp, J. R., Kluge, R., Giesen, K., Plum, L., Radke, P., Hanrath, P., & Joost, H. G. (2000). A metabolic syndrome of hypertension, hyperinsulinaemia and hypercholesterolaemia in the New Zealand obese mouse. *European Journal of Clinical Investigation*, *30*, 195–202. https://doi.org/10.1046/j.1365-2362.2000.00611.x

Penna, C., Andreadou, I., Aragno, M., Beauloye, C., Bertrand, L., Lazou, A., Falcão-Pires, I., Bell, R., Zuurbier, C. J., Pagliaro, P., & Hausenloy, D. J. (2020). Effect of hyperglycaemia and diabetes on acute myocardial ischaemia–reperfusion injury and cardioprotection by ischaemic conditioning protocols. *British Journal of Pharmacology*, *177*, 5312–5335. https://doi.org/10.1111/bph.14993

Percie du Sert, N., Hurst, V., Ahluwalia, A., Alam, S., Avey, M. T., Baker, M., Browne, W. J., Clark, A., Cuthill, I. C., Dirnagl, U., Emerson, M., Garner, P., Holgate, S. T., Howells, D. W., Karp, N. A., Lazic, S. E., Lidster, K., MacCallum, C. J., Macleod, M., … Würbel, H. (2020). The ARRIVE guidelines 2.0: Updated guidelines for reporting animal research. *PLoS Biology*, *18*, e3000410. https://doi.org/10.1371/journal.pbio.3000410

Perricone, A. J., Bivona, B. J., Jackson, F. R., & Vander Heide, R. S. (2013). Conditional knockout of myocyte focal adhesion kinase abrogates ischemic preconditioning in adult murine hearts. *Journal of the American Heart Association*, *2*, e000457. https://doi.org/10.1161/JAHA.113.000457

Pickard, J. M., Davidson, S. M., Hausenloy, D. J., & Yellon, D. M. (2016). Co-dependence of the neural and humoral pathways in the mechanism of remote ischemic conditioning. *Basic Research in Cardiology*, *111*, 50. https://doi.org/10.1007/s00395-016-0568-z

Randriamboavonjy, V., Schrader, J., Busse, R., & Fleming, I. (2004). Insulin induces the release of vasodilator compounds from platelets by a nitric oxide-G kinase-VAMP-3-dependent pathway. *The Journal of Experimental Medicine*, *199*, 347–356. https://doi.org/10.1084/jem.20030694

Rassaf, T., Totzeck, M., Hendgen-Cotta, U. B., Shiva, S., Heusch, G., & Kelm, M. (2014). Circulating nitrite contributes to cardioprotection by remote ischemic preconditioning. *Circulation Research*, *114*, 1601–1610. https://doi.org/10.1161/CIRCRESAHA.114.303822

Rehman, S. U., Schallschmidt, T., Rasche, A., Knebel, B., Stermann, T., Altenhofen, D., Herwig, R., Schürmann, A., Chadt, A., & al-Hasani, H. (2021). Alternative exon splicing and differential expression in pancreatic islets reveals candidate genes and pathways implicated in early diabetes development. *Mammalian Genome : Official Journal of the International Mammalian Genome Society*, *32*, 153–172. https://doi.org/10.1007/s00335-021-09869-1

Reinstadler, S. J., Stiermaier, T., Eitel, C., Metzler, B., de Waha, S., Fuernau, G., Desch, S., Thiele, H., & Eitel, I. (2017). Relationship between diabetes and ischaemic injury among patients with revascularized ST-elevation myocardial infarction. *Diabetes, Obesity & Metabolism*, *19*, 1706–1713. https://doi.org/10.1111/dom.13002

Rizvi, F., Preston, C. C., Emelyanova, L., Yousufuddin, M., Viqar, M., Dakwar, O., Ross, G. R., Faustino, R. S., Holmuhamedov, E. L., & Jahangir, A. (2021). Effects of aging on cardiac oxidative stress and transcriptional changes in pathways of reactive oxygen species generation and clearance. *Journal of the American Heart Association*, *10*, e019948. https://doi.org/10.1161/JAHA.120.019948

Sayour, N. V., Brenner, G. B., Makkos, A., Kiss, B., Kovácsházi, C., Gergely, T. G., Aukrust, S. G., Tian, H., Zenkl, V., Gömöri, K., Szabados, T., Bencsik, P., Heinen, A., Schulz, R., Baxter, G. F., Zuurbier, C. J., Vokó, Z., Ferdinandy, P., & Giricz, Z. (2023). Cardioprotective efficacy of limb remote ischaemic preconditioning in rats: Discrepancy between a meta-analysis and a three-centre in vivo study. *Cardiovascular Research*, *119*, 1336–1351. https://doi.org/10.1093/cvr/cvad024

Schremmer, J., Busch, L., Baasen, S., Heinen, Y., Sansone, R., Heiss, C., Kelm, M., & Stern, M. (2023). Chronic PCSK9 inhibitor therapy leads to sustained improvements in endothelial function, arterial stiffness, and microvascular function. *Microvascular Research*, *148*, 104513. https://doi.org/10.1016/j.mvr.2023.104513

Siragusa, M., & Fisslthaler, B. (2017). Insulin keeps PYK-ing on eNOS: Enhanced insulin receptor signaling induces endothelial dysfunction. *Circulation Research*, *120*, 748–750. https://doi.org/10.1161/CIRCRESAHA.117.310576

Siragusa, M., & Fleming, I. (2016). The eNOS signalosome and its link to endothelial dysfunction. *Pflügers Archiv / European Journal of Physiology*, *468*, 1125–1137. https://doi.org/10.1007/s00424-016-1839-0

Siragusa, M., Thöle, J., Bibli, S. I., Luck, B., Loot, A. E., de Silva, K., Wittig, I., Heidler, J., Stingl, H., Randriamboavonjy, V., Kohlstedt, K., Brüne, B., Weigert, A., Fisslthaler, B., & Fleming, I. (2019). Nitric oxide maintains endothelial redox homeostasis through PKM2 inhibition. *The EMBO Journal*, *38*, e100938. https://doi.org/10.15252/embj.2018100938

Tai, L. K., Okuda, M., Abe, J., Yan, C., & Berk, B. C. (2002). Fluid shear stress activates proline-rich tyrosine kinase via reactive oxygen species-dependent pathway. *Arteriosclerosis, Thrombosis, and Vascular Biology*, *22*, 1790–1796. https://doi.org/10.1161/01.ATV.0000034475.40227.40

Viswambharan, H., Yuldasheva, N. Y., Sengupta, A., Imrie, H., Gage, M. C., Haywood, N., Walker, A. M. N., Skromna, A., Makova, N., Galloway, S., Shah, P., Sukumar, P., Porter, K. E., Grant, P. J., Shah, A. M., Santos, C. X. C., Li, J., Beech, D. J., Wheatcroft, S. B., … Kearney, M. T. (2017). Selective enhancement of insulin sensitivity in the endothelium in vivo reveals a novel proatherosclerotic signaling loop. *Circulation Research*, *120*, 784–798. https://doi.org/10.1161/CIRCRESAHA.116.309678

Yin, G., Yan, C., & Berk, B. C. (2003). Angiotensin II signaling pathways mediated by tyrosine kinases. *The International Journal of Biochemistry & Cell Biology*, *35*, 780–783. https://doi.org/10.1016/S1357-2725(02)00300-X

Zaharia, O. P., Strassburger, K., Strom, A., Bönhof, G. J., Karusheva, Y., Antoniou, S., Bódis, K., Markgraf, D. F., Burkart, V., Müssig, K., Hwang, J. H., Asplund, O., Groop, L., Ahlqvist, E., Seissler, J., Nawroth, P., Kopf, S., Schmid, S. M., Stumvoll, M., … Ziegler, D. (2019). Risk of diabetes-associated diseases in subgroups of patients with recent-onset diabetes: A 5-year follow-up study. *The Lancet Diabetes & Endocrinology*, *7*, 684–694. https://doi.org/10.1016/S2213-8587(19)30187-1

SUPPORTING INFORMATION

Additional supporting information can be found online in the Supporting Information section at the end of this article.

How to cite this article: Erkens, R., Duse, D. A., Brum, A., Chadt, A., Becher, S., Siragusa, M., Quast, C., Müssig, J., Roden, M., Cortese-Krott, M., Ibáñez, B., Lammert, E., Fleming, I., Jung, C., Al-Hasani, H., Heusch, G., & Kelm, M. (2024). Inhibition of proline-rich tyrosine kinase 2 restores cardioprotection by remote ischaemic preconditioning in type 2 diabetes. *British Journal of Pharmacology*, *181*(21), 4174–4194. https://doi.org/10.1111/bph.16483